



The Report is Generated by DrillBit Plagiarism Detection Software

Submission Information

Author Name	Yash Raj Srajan Srivastava
Title	Aerodynamic Investigation of High Performance Glider
Original File Name	329_21647
Submission/Paper ID	180654
Submission Date	09-Nov-2020 11:07:53
Total Pages	59
Total Words	12216

Result Information

Similarity	9 %
Unique	91 %
Journal/Publication Sources	8 %

Exclude Information

References/Bibliography	Not Excluded
Quotes	Not Excluded
Sources: Less than 14 Words Similarity	Not Excluded



DrillBit Similarity Report

9

50

A

SIMILARITY %

MATCHED SOURCES

GRADE

- A-Satisfactory (0-10%)**
- B-Upgrade (11-40%)**
- C-Poor (41-60%)**
- D-Unacceptable (61-100%)**

SL.No	LOCATION	MATCHED DOMAIN	%	SOURCE TYPE
1.	23	American Institute of Aeronautics and Astronautics AIAA International	2	Publication
2.	17	downloads.hindawi.com	<1	Publication
3.	7	The influence of oscillating trailing-edge flap on the dynamic stall c by Seyednia-2019	<1	Publication
4.	14	Effect of interfacial tension gradients on emulsion stability by S-1994	<1	Publication
5.	25	Flow Patterns and Aerodynamic Characteristics of a Wing-Strake Configu by MJLiu-1980	<1	Publication
6.	11	An interactive finite difference preprocessor for three-dimensional fl by C-1981	<1	Publication
7.	9	Tissue growth in a rotating bioreactor. Part I mechanical stability, by Waters, S. L. Cumm- 2006	<1	Publication
8.	26	ftp.demec.ufpr.br	<1	Publication

9. **1** Boundary layer in compressible flow of wet water vapour by Wojciec-1979 <1 Publication
-
10. **18** Thesis submitted to shodhganga - shodhganga.inflibnet.ac.in <1 Publication
-
11. **13** The theory of sonic bangs by CHE-1961 <1 Publication
-
12. **39** journals.plos.org <1 Publication
-
13. **20** Etching of polysilicon in inductively coupled Clsub 2 and HBr discha by A-2002 <1 Publication
-
14. **27** arxiv.org <1 Publication
-
15. **22** IEEE 2013 46th Hawaii International Conference on System Sciences (H by <1 Publication
-
16. **19** SynGAP isoforms exert opposing effects on synaptic strength by McMahon-2012 <1 Publication
-
17. **3** www.doaj.org <1 Publication
-
18. **5** bmcmolcellbiol.biomedcentral.com <1 Publication
-
19. **31** Thesis submitted to Theses and Dissertations <1 Publication
-
20. **33** IEEE 2008 IEEE Workshop on Motion and video Computing (WMVC)- Copp, by Suandi, Shahrel A.- 2008 <1 Publication
-

21. **24** Debt covenant slack and ex-post conditional accounting conservatism by Kim-2019 <1 Publication
-
22. **35** Thesis submitted to shodhganga - shodhganga.inflibnet.ac.in <1 Publication
-
23. **16** Effects of Structural Failure on the Safe Flight Envelope of Aircraft by Nabi-2018 <1 Publication
-
24. **41** Evaluation of mechanical characteristics of nano modified epoxy based by Sindu-215 <1 Publication
-
25. **4** Examining chain bookshops in the context of third place, by Laing, Audrey Royle- 2013 <1 Publication
-
26. **6** myukk.org <1 Publication
-
27. **10** www.cryer.co.uk <1 Internet
-
28. **34** thermalscience.vinca.rs <1 Publication
-
29. **45** A STUDY OF PROMOTIONAL STRATEGIES OF SELECTED FOOD-BASED SUPERSTORES by SOURAV JAIN - 2012 , krishikosh <1 Publication
-
30. **50** www.icci.edu <1 Publication
-
31. **28** Crystallization, structural relaxation and thermal degradation in Pol, by Lizundia, E. Vilas- 2015 <1 Publication
-

32. **30** www.arxiv.org <1 Publication
-
33. **21** Thesis submitted to dspace.mit.edu <1 Publication
-
34. **36** www.atmos-chem-phys-discuss.net <1 Publication
-
35. **15** Problems in the deconvolution of SIMS depth profiles using delta-doped by PC-1993 <1 Publication
-
36. **49** www.researchgate.net <1 Internet
-
37. **46** Applied Computational Aerodynamics Innovation with Computational Ae <1 Publication
-
38. **42** Study on the Curve Shape of C-Shaped Armatures Trailing Arms in Rect, by Deng Feng, Junjia- 2013 <1 Publication
-
39. **12** A discrete gradient-based approach for aerodynamic shape optimisation by M-2006 <1 Publication
-
40. **40** www.arxiv.org <1 Publication
-
41. **37** epljournal.edpsciences.org <1 Internet
-
42. **2** www.jotform.com <1 Internet
-
43. **43** Experimental investigation of wing-in-ground effect with a NACA6409 se by Kwan-2008 <1 Publication
-
44. **38** naac.smsvaranasi.com <1 Publication

45. **8** www.researchgate.net <1 Internet
-
46. **48** www.agroengineering.org <1 Publication
-
47. **29** apem-journal.org <1 Publication
-
48. **44** worldwidescience.org <1 Internet
-
49. **32** publichealthreviews.biomedcentral.com <1 Publication
-
50. **47** www.researchgate.net <1 Internet
-

Minor Project Report on

Aerodynamic Investigation of High-Performance Glider

Submitted To:

Guide: Prof. J.K. Jain

Co-Guide: Prof. Jayanta Sinha

Submitted By:

Yash Raj
A37100417006
B.Tech. + M.Tech. (AE) – Intg.

Srajan Shrivastava
A37100417005
B.Tech. + M.Tech. (AE) – Intg.

TABLE OF CONTENTS

S. No.	Topic	Page No.
1	Introduction	6
2	Glider Performance	7
2.1	Factors Affecting Performance	7
2.1.1	Altitude	7
2.1.2	Temperature	7
2.1.3	Wind	7
2.1.4	Weight	7
2.2	Rate of Climb	7
2.3	Placards	8
2.4	L/D Ratio	8
2.5	Ballast	8
3	Glider Aerodynamics	9
3.1	How gliders stay aloft for long period of time?	9
4	Types of Gliders	10
5	Evolution of Aerofoils	11
6	Drags and their contributions	17
6.1	Induced drag	18
6.2	Profile Drag	19
6.3	Fuselage Drag	20
7	Modern Sailplanes	21
8	Diana 3 Sailplane	22
8.1	MATLAB Code Analysis (Diana 3)	23
8.2	Output	27
8.3	Figures	27
9	ASW 22 BL Sailplane	29
9.1	MATLAB Code Analysis (ASW 22 BL)	30
9.2	Output	35
9.3	Figures	35
10	Verification of MATLAB Results	38
10.1	Analysis	39
11	Ansys Simulations	40

11.1	Steps	40
11.2	Results	41
12	Verification of Ansys Simulations	48
12.1	Analysis	49
13	Lift and Drag Coefficients at different chord length	50
13.1	Results	50
13.2	Analysis	54
14	Conclusion	55
15	Contributions	56
15.1	Individual contribution report by Yash	56
15.2	Individual contribution report by Srajan	58

LIST OF TABLES

Table No.	Title of the Table	Page No.
1	Types of gliders	10
2	Comparison of MATLAB Results and Glider Manual Results	38
3	C_l and C_d values with corresponding α	47
4	Comparison of Simulation Results and XFOIL Results	48
5	C_l and C_d at different chord length	54

LIST OF FIGURES

Figure No.	Caption of the Figure	Page No.
1	Aerofoil geometric shape of a Lilienthal glider	11
2	C_l and C_d curve of Lilienthal aerofoil	11
3	C_l and C_m vs Alpha curve of Lilienthal aerofoil	11
4	Aerofoil geometric shape of the Goe441 of the Vampyr	12
5	C_l and C_d curve of Goe441 aerofoil for fully turbulent boundary layer	12
6	C_l and C_m vs Alpha curve of Goe441 aerofoil for fully turbulent boundary layer	12
7	Aerofoil geometric shape of the NACA 633618 of the Ka6	13
8	C_l and C_d curve for laminar and turbulent boundary	13

	layer of the NACA 633618 aerofoil	
9	Aerofoil geometric shape of the Eppler EC86(-3)-914 used for the Phoenix	14
10	Cl and Cd curve for laminar boundary layer of the Eppler EC86(-3)-014 and NACA 633618 aerofoil	14
11	Aerofoil geometric shape of the FX 61-163 of ASW-15	15
12	Cl and Cd curve for the aerofoils EC 86(-3)-914 and FX 61-163	15
13	Cl and Cm vs Alpha curve for the aerofoils EC 86(-3)-914 and FX 61-163	15
14	Aerofoil geometric shape of the aerofoil FX 62-K-131/17(D36)	16
15	Cl and Cd curve behavior for the aerofoils FX 62-K-131/17 and FX 61-163	16
16	Speed polar contribution curve of the ASW-27	17
17	Wing geometry with Winglets	18
18	Wing geometry without winglets	18
19	k vs Cl curve of wings with winglets and without winglets	18
20	Pressure distribution of aerofoil with 0° flap	19
21	Pressure distribution of aerofoil with 20° flap extended	19
22	Pressure distribution on a fuselage with cockpit extension	20
23	Sailplane Diana-3	21
24	Sailplane ASW 22 BL	21
25	Diana 3	22
26	Technical parameters of Diana 3	22
27	L/D vs. KCAS	27
28	L/D vs. TAS	28
29	$(L/D)_{\max}$	28
30	Parasite, induced, and total drag curves	29
31	Drag Polar	29
32	ASW 22 BL Sailplane	30
33	Technical Data of ASW 22 BL Sailplane	30

34	L/D vs. KCAS	35
35	L/D vs. TAS	36
36	$(L/D)_{\max}$	36
37	Parasite, induced, and total drag curves	37
38	Drag Polar	37
39	ASW 22 BL Factory Speed Polar	38
40	Static pressure contour at $\alpha = 0^\circ$	41
41	Velocity contour at $\alpha = 0^\circ$	41
42	Static pressure contour at $\alpha = -12^\circ$	42
43	Velocity contour at $\alpha = -12^\circ$	42
44	Static pressure contour at $\alpha = -9^\circ$	43
45	Velocity contour at $\alpha = -9^\circ$	43
46	Static pressure contour at $\alpha = -6^\circ$	43
47	Velocity contour at $\alpha = -6^\circ$	44
48	Static pressure contour at $\alpha = -3^\circ$	44
49	Velocity contour at $\alpha = -3^\circ$	44
50	Static pressure contour at $\alpha = 3^\circ$	45
51	Velocity contour at $\alpha = 3^\circ$	45
52	Static pressure contour at $\alpha = 9^\circ$	45
53	Velocity contour at $\alpha = 9^\circ$	46
54	Static pressure contour at $\alpha = 15^\circ$	46
55	Velocity contour at $\alpha = 15^\circ$	46
56	Static pressure contour at $\alpha = 18^\circ$	47
57	Velocity contour at $\alpha = 18^\circ$	47
58	Static pressure contour at AR = 38.3	50
59	Velocity contour at AR = 38.3	50
60	Static pressure contour at AR = 42	51

61	Velocity contour at AR = 42	51
62	Static pressure contour at AR = 35	52
63	Velocity contour at AR = 35	52
64	Static pressure contour at AR = 32	53
65	Velocity contour at AR = 32	53

1. Introduction

A glider or a sailplane is just another type of a fixed wing aircraft. Generally, they are used in the sport of gliding. This idea of flying gliders for sport was originated in Germany in 1910. Consequently, world's largest sailplane production company Alexander Schleicher GmbH & Co. is located in Poppenhausen, Germany.

The major difference between a sailplane and a conventional aircraft is engines. A sailplane lacks engine and that's why there isn't any forward force or thrust acting on the glider. As there is no thrust, force of drag goes unopposed which quickly brings the glider down. Therefore, while designing a sailplane, the most important thing that designing engineers have to keep in mind is to minimise drag as much as possible.

In this project, we have firstly discussed the basic aerodynamics of the glider and external factors that affects the performance of the glider. A section in this report is also dedicated to the evolution of aerofoils that are used while designing the wing of sailplane. This will shed some light on how the design of sailplanes and aerofoils has changed with the passage of time and how it can only get better.

But the main topic of this report is to analyse the performance of gliders. There are two sailplanes whose performance we are going to analyse: Diana 3 and ASW 22 BL.

Diana 3 is the most modern sailplane which was designed in 2018. We have calculated its best glide data, that is, best gliding speed, glide ratio, sink rate, angle of gliding, etc. These values are the values at which Diana 3 sailplane should fly for the maximum performance. We have done the same for ASW 22 BL sailplane also and then compared these results with the actual results. Since Diana 3 is a modern sailplane, we cannot verify each and every value that was calculated, however, we can compare the most important parameter, which is glide ratio. In case of ASW 22 BL, we can compare every parameter that we calculated because the actual values of those parameters can be found easily.

Lastly, we have done turbulence testing of the aerofoil DU 84-132 that is used in ASW 22 BL sailplane with Ansys and found the values of coefficient of lift and drag at various angle of attacks. For verification of these simulations, we compared our results with the database of aerofoiltools.com. This turbulence testing is done at Reynolds number of 1,000,000. We have also found values of drag and lift coefficients at different chord length of the aerofoil and got some really interesting results.

2. Glider Performance

2.1 Factors Affecting Performance

Sailplane performance during flight depends on many external atmospheric conditions. These are altitude, temperature and wind. The only important performance parameter that can be controlled is weight of the sailplane during designing. These factors are explained in detail below:

2.1.1 Altitude

Density of air decreases as we go above the surface of the earth⁹ because at high altitudes, atmospheric pressure acting on the air decreases and molecules of the air can easily move further apart. As a result, number of molecules in the same volume of air will be lower than that at lower altitudes. As the density is reduced, the lift generated on the sailplane will also be reduced and hence sailplane's take-off and climb performance is reduced.

2.1.2 Temperature

As the temperature increases, distance between molecules will also increase due to thermal expansion. Therefore, increasing the temperature will have similar effects on the performance of the sailplane as increasing the altitude, that is, as temperature increases, take-off and climb performance is reduced.

2.1.3 Wind

Wind can affect the sailplane performance severely. During launch, headwind will decrease the take-off distance while tailwind will increase the take-off distance. And if there are crosswinds, proper controlling and correction procedure for sailplane heading is required for successful take-off. At the time of cruising flight, headwinds reduce the speed of the sailplane. For example, if the sailplane is flying at 20 m/s, and a headwind of 5 m/s appears, then the net speed will be 15 m/s. On the other hand, tailwind increase the speed of the sailplane. If in the previous example, a tailwind of 5 m/s appears, then the net speed would become 25 m/s. Crosswinds during cruise phase have similar effects as in launch phase. It changes the sailplane heading due to which it needs to be corrected. It must be noted that crosswinds have some headwind or tailwind component which can also increase or decrease the speed of the sailplanes. During landing, these wind effects must be taken into account and corrections and allowances must be made for the same.¹³

2.1.4 Weight

An important design parameter of the sailplane is obviously its weight. All other characteristics like lift, drag, and glide ratio of the sailplane are impacted solely by its design and construction, and can be predetermined at take-off. The only characteristic the pilot controls is the weight of the sailplane. In some cases, pilots can also control glider configurations with the help of flaps.¹⁵ However, flaps are not available in all the models of sailplanes. Therefore, weight is the only other characteristic that can be controlled. While it is true that increased weight won't be helpful during take-off and climb phase, but during cruise phase, a pilot can increase the net forward force by increasing the weight of the glider which ultimately increases the speed of the sailplane. During launch phase, a heavy glider would require more take-off distance to reach flying speed because a heavy glider has more inertia, which proves to be a problem while accelerating the sailplane. Due to similar reasons, the heavier sailplane takes longer to climb than the lighter glider.¹⁷

2.2 Rate of Climb

Rate of climb directly depends on the ground-launching equipment for ground launching gliders. The greater the strength of ground launching equipment, the higher the rate of climb will be. When ground launching, value of rate of climb can surpass 2,000 feet per minute (fpm) if the winch of the tow vehicle is powerful ¹⁸ and the speed of the tow vehicle is high. When aerotowing, rate of climb is dependent on the power of the towplane. Therefore, it is important to select a high-performance tow vehicle to achieve high rate of climb.

2.3 Placards

Cockpit placards are like quick steps guides for pilots. These provide information regarding the safe operation of the glider to a pilot. All required placards are in the Glider Flight Manual/Pilot's Operating Handbook (GFM/POH). If the design of the glider is very complex, then the amount of information provided in placards is also high and difficult to read. For example, a high-performance sailplane may be equipped with wing flaps, retractable landing gear, a water ballast system, and other features to optimise the performance of that sailplane. In such cases, it may require additional placards.

2.4 L/D Ratio

L/D ratio is the ratio of lift to drag. Value of this ratio is equal to the glide ratio. A glide ratio tells the horizontal distance covered by the sailplane per unit of altitude lost. For example, if a sailplane have the glide ratio of 50, then it will cover 50 feet of horizontal distance while losing 1 feet of altitude. While designing a sailplane, the objective is to make this value as high as possible.

2.5 Ballast

Ballast is non-structural weight that is added to a glider. In sailplanes, there are two ways in which ballast weight can be used. Trim ballast can be used to alter the CG of the glider and ³ thus making the handling of the sailplane according to the requirement of the pilot. Another type of ballast is performance ballast which is loaded into the sailplane which can improve the high-speed cruise performance.

3. Glider Aerodynamics

When we talk about conventional aircraft, there are four forces acting on it during steady and level flight. These are lift, weight, thrust, and drag. Lift counters gravity or weight force, while drag counters the forward force called thrust. During steady level flight, lift is equal to weight. Sailplanes which have engines installed can easily obtain thrust from that engine. So, during gliding, a pilot can switch on or switch off the engine according to the requirement. But what about the engineless sailplanes. They can glide for hours without any engine. So where does the thrust come from. The answer is that a sailplane uses the horizontal component of weight and lift to produce this forward force. That is the reason why the weight of sailplane is increased during gliding with the help of water ballast. That is also one of the reasons to maximise L/D ratio while designing the sailplane.

3.1 How Gliders stay aloft for long period of time?

We now know that while designing a sailplane, we attempt to maximize the L/D ratio for optimised performance. But that is not the only way for a sailplane to fly for hours. Pilot can also take advantage of the external factors. There are four kinds of convection (rising air); *thermals, ridge lift, standing mountain waves, and convergence lift*. Pilots can also make use of them in order to generate more lift in a sailplane. A thermal is created when the heat is absorbed by the ground from the sun. A column of hot and humid air rises from the ground which is used by the sailplane pilots to create lift. Thermals can make sailplanes reach altitudes of up to 18000 fts, but generally a rise 5000-6000 ft is observed. Ridge lifts are generated when high-speed wind strikes the irregular surface like cliffs and mountains. Air will try to flow past them by flowing above them and while doing so, provides lift to the sailplane pilots. Wave lift is the consequence of oscillatory motion of air. It is also called gravity waves by atmospheric scientists. These provides maximum altitude gain out of the three. Sailplanes can reach altitudes of as high as 45000 fts. For instance, the cited altitude record below was achieved in such a wave. Convergence lift is generated when two masses of air flowing in different directions collide, like sea-breeze and inland air mass. Such conditions generally exist near the ground between valleys of ocean waves or on the leeward side of ridges. The wind speed in the upper air mass is much greater when compared to the lower one and the two are separated by a steep speed gradient.

4. Types of Gliders

Table 1: Types of gliders

	Paraglider	Hang glider	High Performance Gliders/Sailplanes
Undercarriage	Pilot's legs used for take-off and landing	Pilot's legs used for take-off and landing	Wheeled undercarriage or skids are used
Wing Structure	Entirely flexible	Generally flexible but supported on a rigid frame	Rigid wing surface which totally encases wing structure
Speed Range (stall speed-max speed)	Slower- typically 25-60 km/h hence easier to launch	Comparatively faster (up to 20-75 km/h)	Max speed up to 280km/h and stall speed up to 65km/h
Max Glide Ratio	About 10 relatively poor glide performance	About 17 with up to 20 for rigid wings	Typically, around 60 but for 15-18 m span GR between 30 to 60
Turn Radius	Tighter turn radius	Somewhat larger turn radius	Even greater turn radius but still able to circle tightly in thermals
Cost	For a brand new one, the cost is around 1,50,000 INR	2,75,000 INR (Data shown is for Aeros Fox 16)	2,00,00,000 INR for new and for used it is around 15Lakhs to 40Lakhs

5. Evolution of Aerofoils

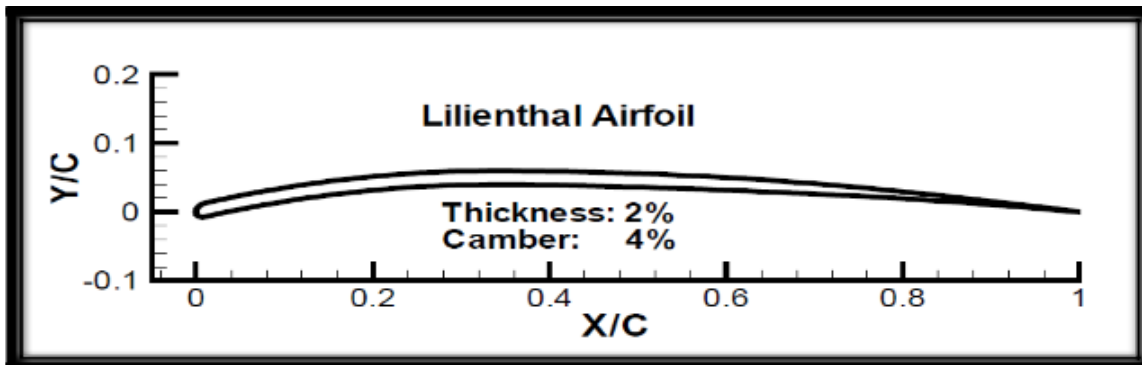


Fig 1: Aerofoil geometric shape of a Lilienthal glider

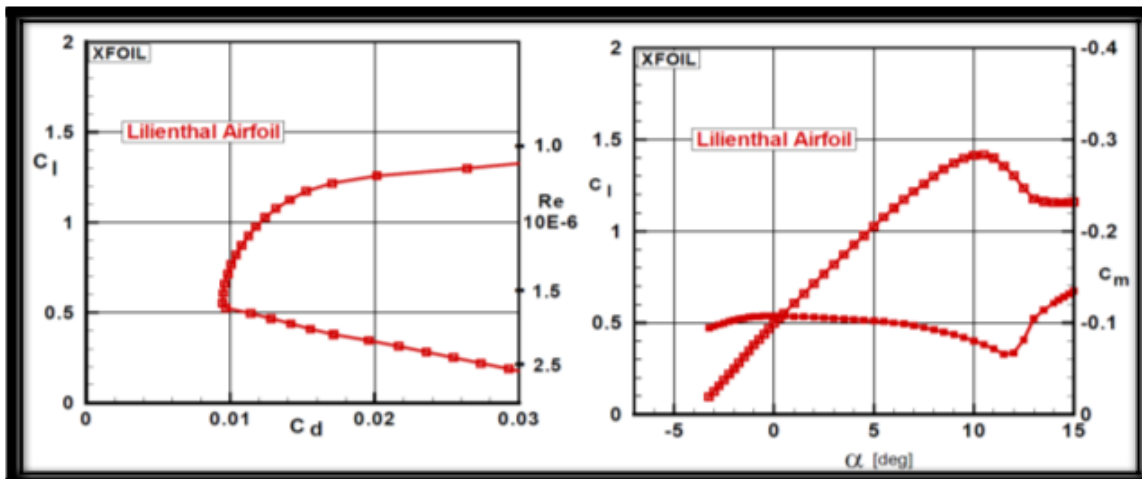


Fig 2: C_l vs C_d curve of Lilenthal aerofoil

Fig 3: C_l and C_m vs α curve of Lilenthal aerofoil

²¹ Found in the year 1894, Lilenthal aerofoil was the first glider aerofoil invented by a scientist named Lilenthal. It covered a distance of 80m from a height of 15m. Although it has been a big achievement ²² but there were some issues regarding the lift and moment curves. In the coefficient of lift vs coefficient of drag curve, below coefficient of lift of 0.5 there was a rapid increase in coefficient of drag which clearly indicated a separation of flow over the lower side of aerofoil. In lift and moment characteristics curves, there was also the lift breakdown at alpha of 15 degrees.

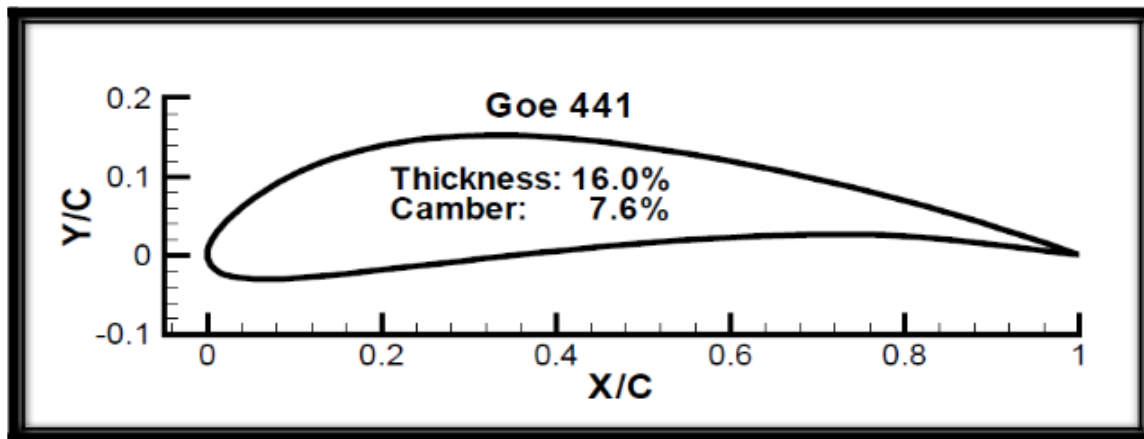


Fig 4: Aerofoil geometric shape of Goe441 of the Vampyr

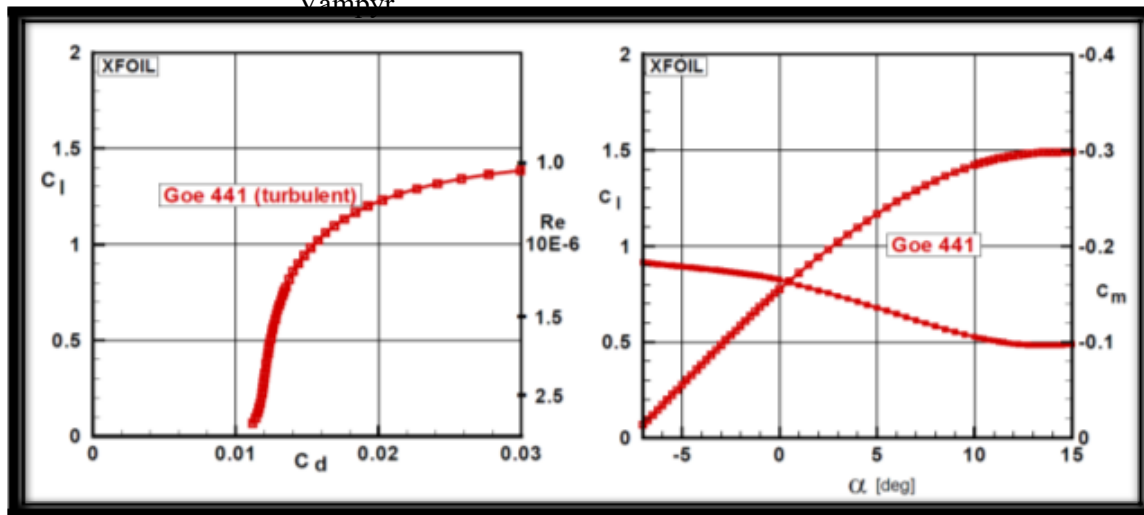


Fig 5: C_l vs C_d curve of Goe441 aerofoil for fully turbulent boundary layer

Fig 6: C_l and C_m vs α of Goe441 aerofoil for fully turbulent boundary layer

Goe441 aerofoil represented the Vampyr sailplane invented in the year 1921 by Academics Flying Group. In this case in lift and moment characteristics curve, there was also the lift breakdown at 15degrees. And in coefficient of lift vs coefficient of drag curve, at coefficient of lift of almost equal to 0, there was already the drag present.

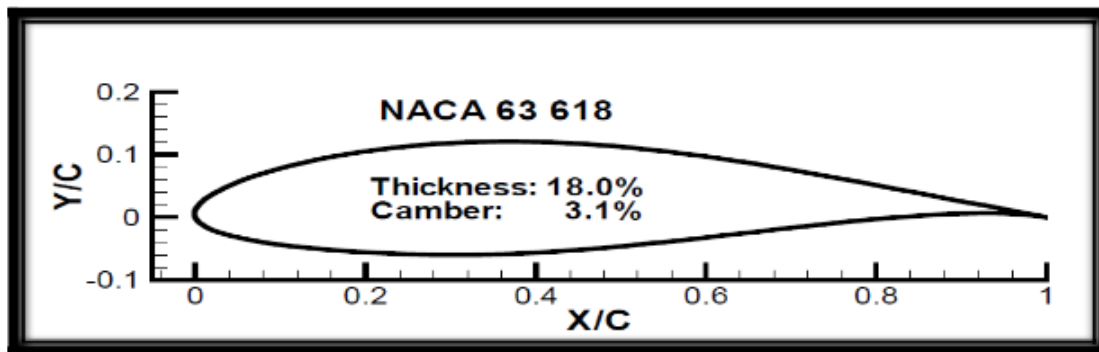


Fig 7: Aerofoil geometric shape of the NACA 633618 of the Ka6

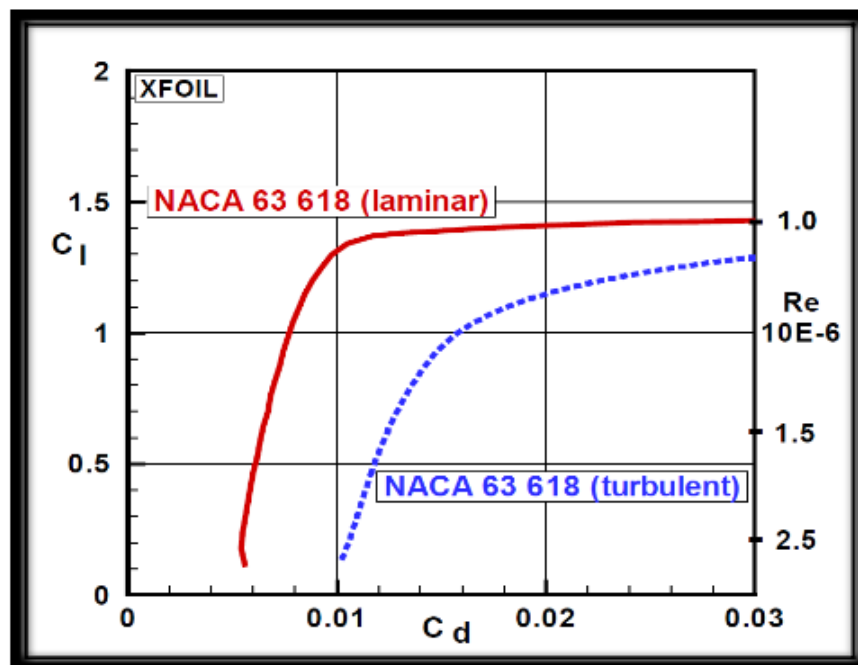


Fig 8: C_l vs C_d curve for laminar and turbulent boundary layer of the NACA 633618 aerofoil

Up till now all the aerofoils were developed for fully turbulent boundary layer but during the 1940s the concept of laminar aerofoils came into being. The NACA 633618 which was developed in the year 1938, its wings required an extremely low surface roughness and an accurate shape of the aerofoil contour. It was difficult to achieve with the wooden kind of structure in the early fifties but further due to weight the torsion D-box was strained to less than the first 30% of wing chord followed by a covering, clearly terminating the laminar boundary layer. In the coefficient of lift vs coefficient of drag curve, the drag polar shifted toward left for laminar boundary layer resulting in loss of drag which a great achievement at that time.

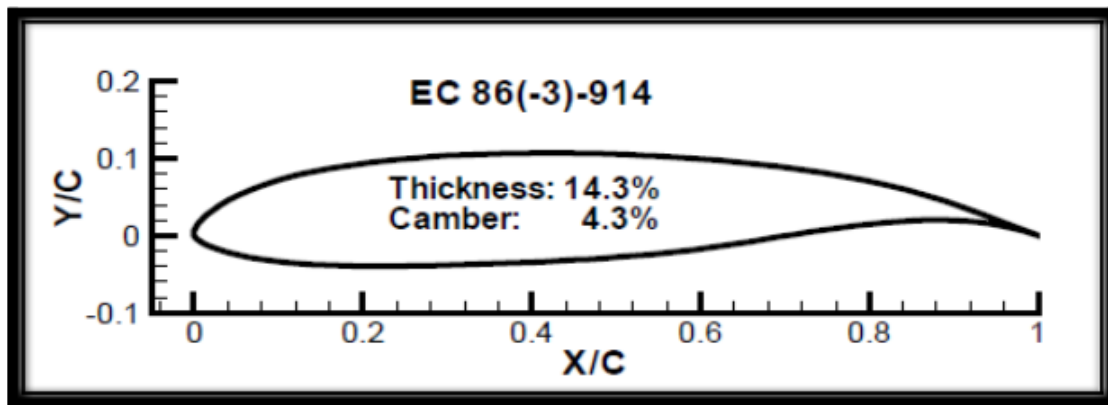


Fig 9: Aerofoil geometric shape of the Eppler EC86(-3)-914 used for the Phoenix

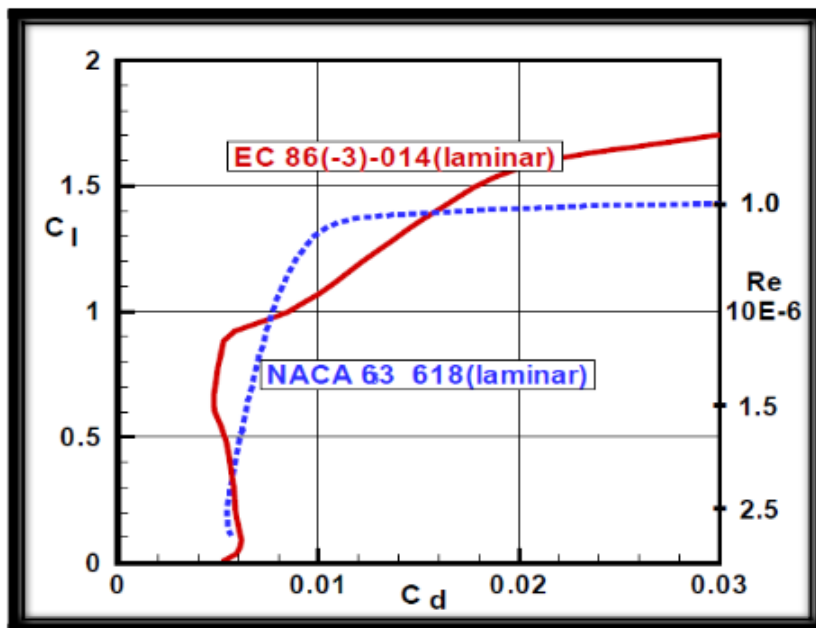


Fig 10: C_l vs C_d curve for laminar boundary layer of the Eppler EC86(-3)-014 and NACA 633618 aerofoil

²³ In the late fifties a new type of construction came up: the technology of the fiberglass composite structure. It allowed to create an accurate shape of the wing with a smooth surface. R. Eppler was the first using the potential of this technology when he designed the “Phoenix” in the year 1957. The maximum lift coefficient was a result of the large curvature ²⁵ on the rear of the upper aerofoil side which was fixing the flow separation within the high curvature region up to very large ²⁶ angles of attack. The very low drag at lift coefficients from 0.5 to 0.9 ⁹ is a result of the long extent of laminar flow on both sides of the aerofoil. At higher and lower lift coefficients the drag is increasing due to reduced ²³ extent of laminar flow on the upper side respectively on the lower side of the aerofoil.

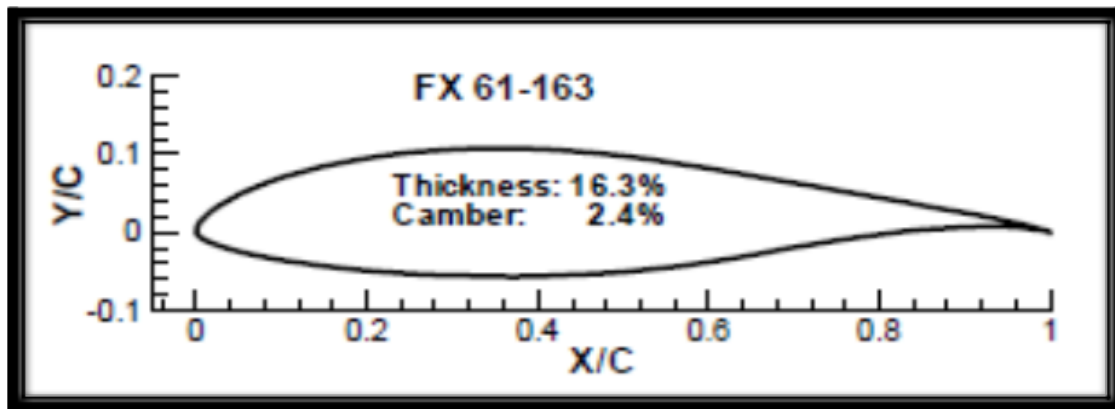


Fig 11: Aerofoil geometric shape of the FX 61-163
of ASW-15

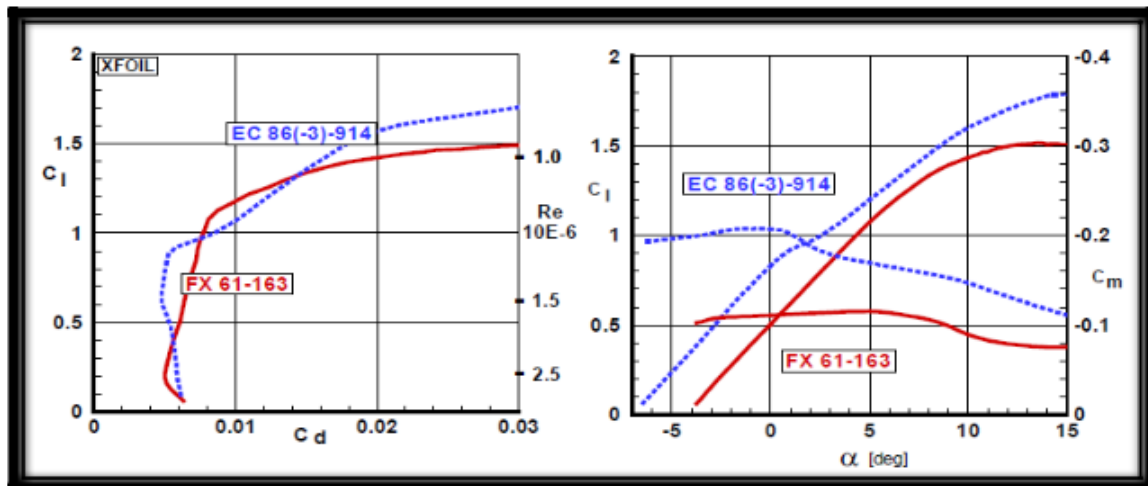


Fig 12: C_l vs C_d curve for the aerofoils EC 86(-3)-914 and FX 61-163

Fig 13: C_l and C_m vs α for the aerofoils EC 86(-3)-914 and FX 61-163

A very successful and appreciable work on aerofoil design and testing had been performed by F. X. Wortmann and D. Althaus. One of their first well known aerofoils is the FX 61-163, designed in 1961. At cruise condition a clear advantage is visible but at medium lift coefficients there was the higher drag compared to the Phoenix aerofoil which can result in a decreased maximum glide ratio.

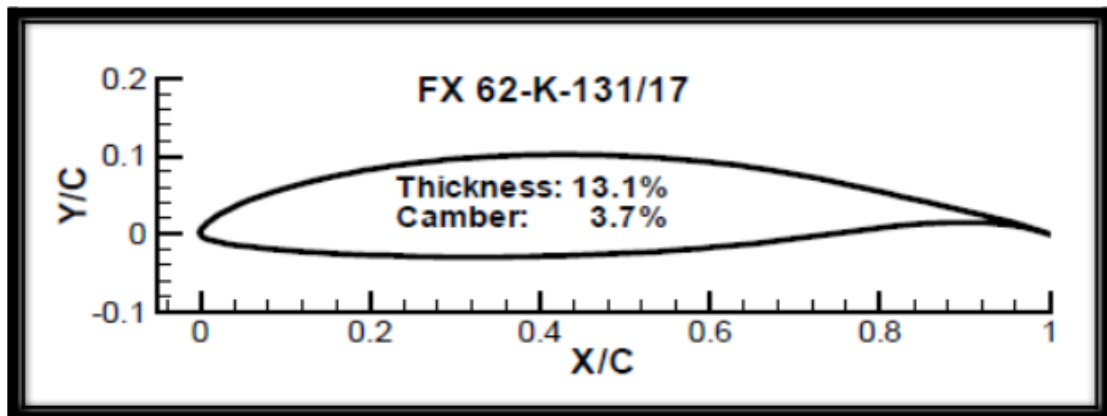


Fig 14: Aerofoil geometric shape of the aerofoil
FX 62-K-131/17(D36)

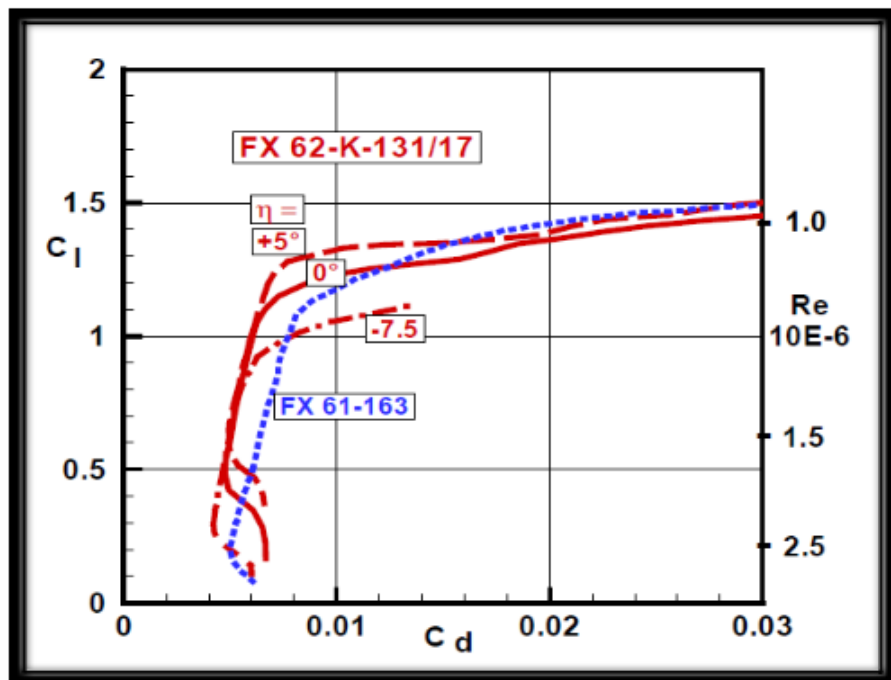


Fig 15: C_l vs C_d curve for the aerofoils FX 62-K-131/17 and FX 61-163

The Wortmann aerofoil FX 62-K-131/17, is one of the early camber flap aerofoils used for the first time at D 36 of the Academic Flight Group of Darmstadt and later with slight modifications and improvements in many other sailplanes. The coefficient of lift vs coefficient of drag curve shows the typical effect of flap deflection on the laminar drag bucket and also the very low drag of this aerofoil with values below 0.005 for cruise conditions.

6. Drags and their contributions

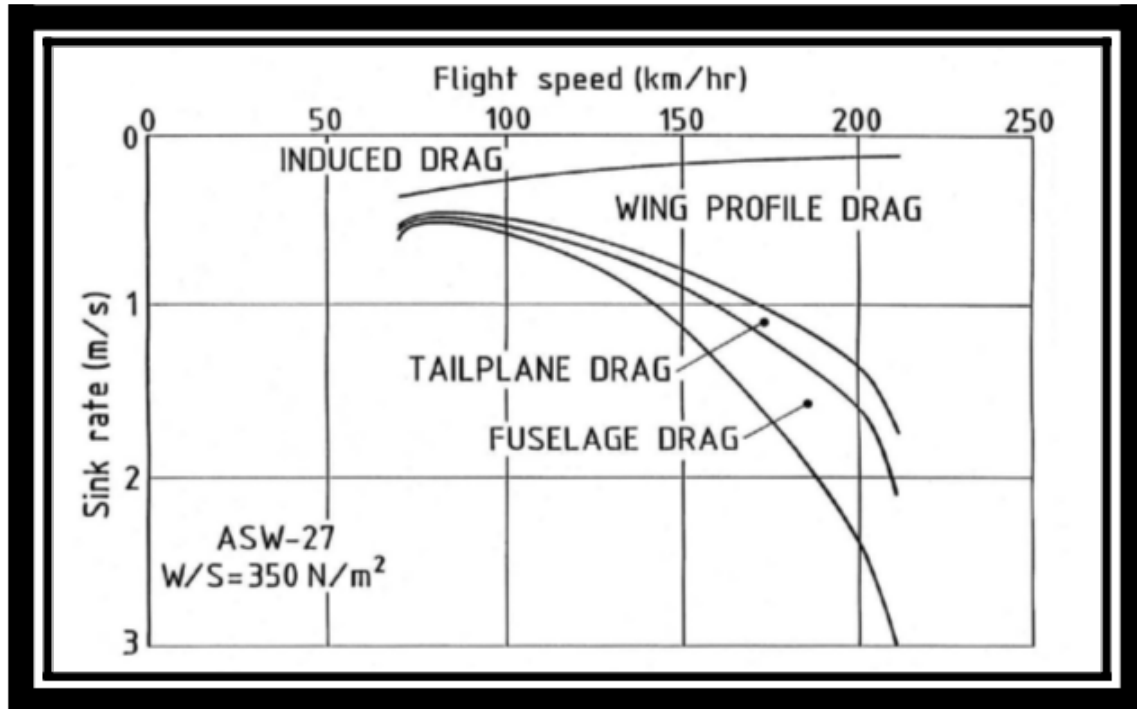


Fig 16: Speed polar contribution curve of the ASW-27

²⁷ Following figure shows the speed polar curve of the ASW-27 sailplane with the contributions of different ²⁸ drags, i.e., induced drag, wing profile drag, tailplane drag, and fuselage drag. the largest contribution is due to the wing; at low speed due to induced drag and at high speed due to profile drag.

6.1 Induced Drag

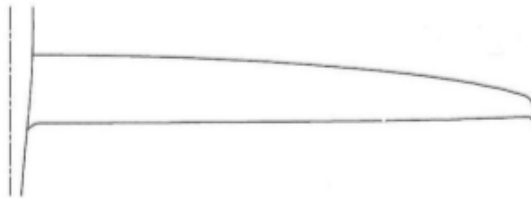


Fig 17: Wing geometry with Winglets

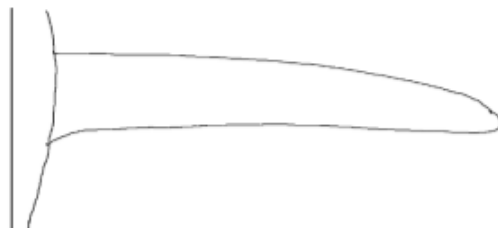


Fig 18: Wing geometry without winglets

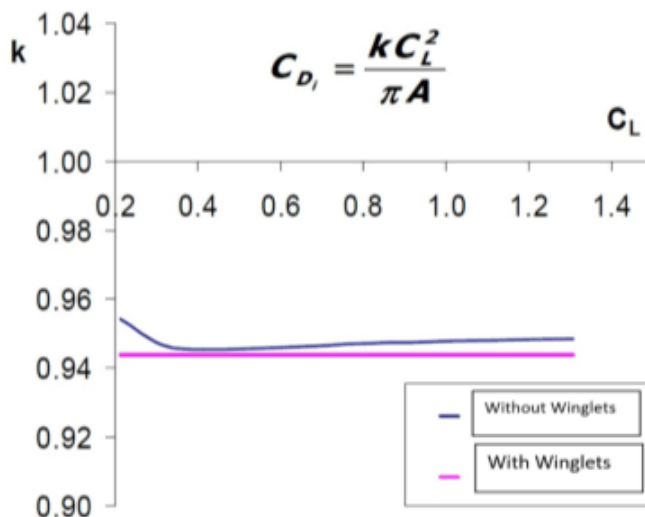


Fig 19: k vs C_L curve of wings with winglets and without winglets

Induced drag has ²⁹ been minimized or decreased ²⁵ by optimizing the wing planform with integrated winglets. The upper two figures show the wing with and without winglets. Winglets makes it difficult for air to flow from lower surface to upper surface since the area of the wing increases. Hence, there is a small pressure difference which results in less induced drag.

²⁷ The below figure shows the absolute minimum induced drag can be realized within 0.96% at all lift coefficients. Apart from that, the winglet aerofoils have been designed for low profile drag in their operational region of lift coefficients, obtained by 100% fully laminar flow on the ⁷ lower surface and 50% on the upper surface of the aerofoil. Also, the ample reserve to separation for yaw has been applied, at significantly low speeds while circling in thermals.

6.2 Profile Drag

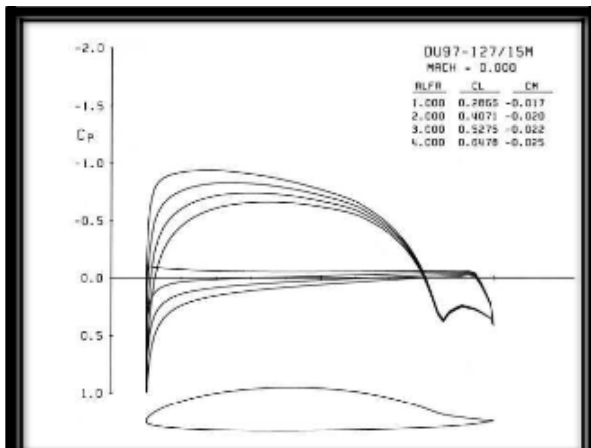


Fig 20: Pressure distribution of aerofoil with 0° flap

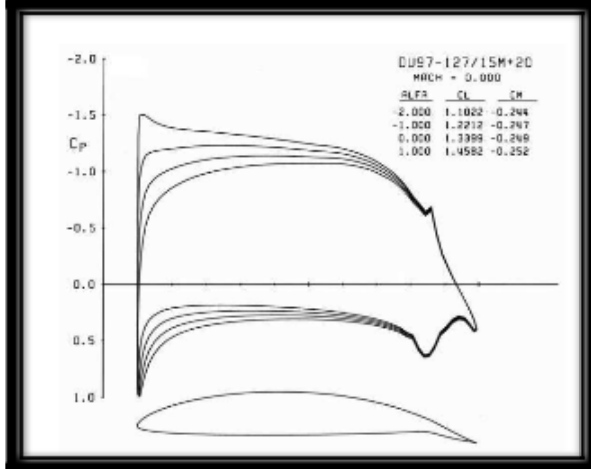


Fig 21: Pressure distribution of aerofoil with 20° flap extended

26 Profile drag is caused by the separation of boundary layer **14** resulting into wakes formation. It depends on the extent of the laminar boundary layer on the lower and upper surfaces of the aerofoils and on aerofoil thickness. The wing aerofoil has laminar flow up to 95% of the chord on the lower surface at the high-speed 0° flap deflection, and up to 75% of the chord on the upper surface at the low-speed 20° flap deflection, as indicated by the pressure distributions in the above figure. The lower and upper surface flap gaps have been sealed by flexible mylar strips. It allows and permits the boundary layer on the lower surface to remain laminar beyond the flap hinge position at the 0° flap deflection up to 95%. On the upper surface the sealing prevents low-pressure peaks and subsequent steep pressure gradients on the flap at 20° deflection, thus postponing separation. Consequently, the profile drag becomes very low over a large range of lift coefficients.

6.3 Fuselage Drag

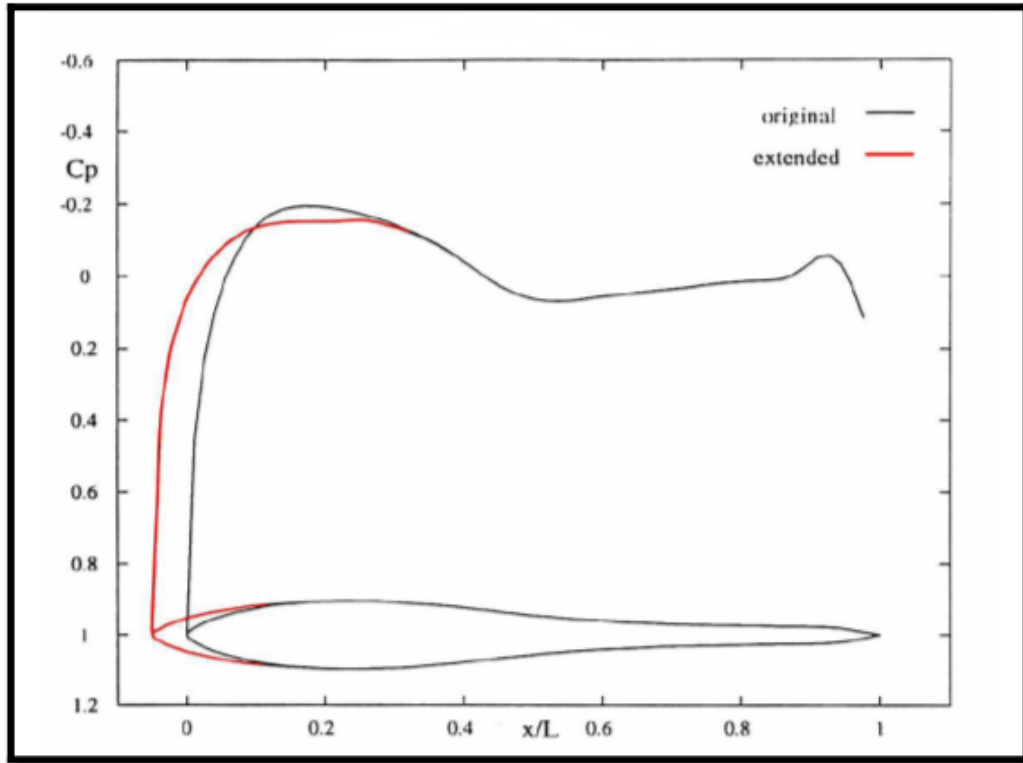


Fig 22: Pressure distribution on a fuselage with cockpit extension

Fuselage drag as clear by its name depends mainly on fuselage thickness, contraction behind the cockpit, and streamline shaping. Fuselage frontal area should be very minimal. Contraction behind the cockpit and the corresponding pressure gradient is restricted because of flow separation when the boundary layer on the fuselage is completely turbulent, for example when flying in rain with heavy thunderstorms. For an undisturbed boundary layer development, continuity of curvature is required in flow direction. It is guaranteed by deriving the top, bottom, and line of largest width from aerofoil shapes.

30 A significant finding is that the fuselage length can be increased by 0.3 metres without any drag increase, as illustrated by the accumulative development of the drag coefficient on a rotationally symmetrical body in the figure. Transition occurs at 33% of the original fuselage length, and thus the total drag is found at the tail. This result grants the probability for improved crashworthiness measures as a longer crumpling nose cone and keeping the pilot's feet out of this zone.

7. Modern Sailplanes



Fig 23: Sailplane Diana-3



Fig 24: Sailplane ASW 22
BL

Modern sailplanes came into effect when we were fully capable of being familiar with the uses of flaps and laminar boundary flow, the reduction of drags and drag coefficient factor, using elliptical wings to ensure minimum drag. Now, we can achieve a glide ratio of as high as 50 and even beyond that.

32 The above figures show the Diana-3 and ASW-22BL sailplanes. These are the sailplanes which we considered, had a look into it and studied and researched into. We did an analysis using MATLAB and Ansys Workbench to determine its performance parameters on both the sailplanes. Though we got the data of aerofoil of only the ASW-22BL sailplane, we also did the simulation analysis, figuring out the turbulence model and also got the curves of C_l vs alpha of that sailplane.

The detailed analysis is presented in the remaining document.

8. Diana 3 Sailplane



Fig 25: Diana 3

Diana 3	
TECHNICAL PARAMETERS	
WING SPAN	18 M
WING AREA	10,456 M ²
ASPECT RATIO	31,15
LENGTH	6,43 M
HEIGHT	1,3 M
EMPTY WEIGHT - PURE GLIDER	306 KG
EMPTY WEIGHT - FES	351 KG
MTOW	600 KG
MAX WING LOADING	57,4 KG/M ²
MIN WING LOADING	37,7 KG/M ²
WATER BALAST	UP TO 240 L
VNE	270 KM/H
STALL SPEED	70 KM/H
MAX SPEED IN ROUGH AIR	220 KM/H
MIN SINK RATE	0,495 M/S AT 73 KM/H
MAX GLIDE RATIO	54 AT 124 KM/H (600 KG)

Fig 26: Technical parameters of Diana 3

Diana-3 sailplane was developed in the year 2018 including a new design of fuselage from Czech manufacturer KKB and a wing from Diana Sailplanes for the 18-metre class span. It was created to achieve highest standard of aerodynamic design. Its performance characteristics in the air is to be better than any 18-metre class sailplane. It has a very high gliding ratio of higher than 50 giving the pilot the comfort of the flight. New Diana 3's wing profile is high-tech mile

step into the future thanks to nowadays simulation software. All in all, it is an aerodynamic masterpiece

8.1 MATLAB Code Analysis (Diana 3)

```
clc; clear; close all;

%%Given parameters of Diana3 sailplane
s = 59.0551; %Wing Span, ft. The wingspan of a glider or an
airplane is the distance from one wingtip to the other wingtip.
S = 112.547447; %Wing 17 area, ft^2, The wing area is a projected area
of the planform bounded by leading and trailing edges and the wingtips
and is almost half of the total surface area.
A = 31.15; %Aspect Ratio, Aspect Ratio of a wing is defined to
be the square of the span divided by the wing area
l = 21.0958; %Length, ft, It is the length of fuselage of a
glider
H = 4.26509; %Height, ft, It 33 is the vertical distance from
bottom of the glider to the top of the glider
WSmax = 11.75645; %Max wing loading, lbs/ft^2, Total mass of an
aircraft divided by the area of its wingtip
WSmin = 7.721569; %Min wing loading, lbs/ft^2, Total mass of an
aircraft divided by the area of its wing root
Vs = 63.7941; %Stall Speed, ft/s, Stall speed is the slowest
speed an aircraft can fly to maintain level flight
Vmax = 200.496; %Max speed in rough air, ft/s, Max speed during
cruise flight
We = 674.615; %Empty weight of glider, lbs
W = 1322.77; %Total weight of glider, lbs
C_D0 = 0.007906; %Parasite drag coefficient, Coefficient of parasitic
drag
e = 1; %Oswald Efficiency Factor, The Oswald efficiency,
similar to the span efficiency, is a correction factor that represents
the change in drag with lift 20 of a three-dimensional wing or airplane, as
compared with an ideal wing having the same aspect ratio and an
elliptical lift distribution.
Clmax = 1.7; %Max lift coefficient
Clmin = -0.1; %Min lift coefficient

%%Set the current conditions for sailplane
h = 1000; %Altitude, ft, It is the vertical distance of the
sailplane above the terrain over which it is flying
phi = 0; %Bank Angle, deg, The bank angle is the angle at
which the vehicle is inclined 9 about its longitudinal axis with respect to
the horizontal.

%%Convert altitude to meters using convlength
h_m = convlength(h,'ft','m');

%%Calculate atmospheric parameters based on altitude using atmoscoesa
[T, a, P, rho] = atmoscoesa(h_m, 'Error'); %These values are absolute
temperature, speed of sound for the input geopotential altitude,
pressure, and density.

%%Convert density from metric to English units using convdensity
rho = convdensity(rho,'kg/m^3','slug/ft^3');

%%Calculate Best Glide Data
```

```

%%The true airspeed (TAS; also KTAS, for knots true airspeed) of an
aircraft is the speed of the aircraft relative to the airmass in which
it is flying.
TAS_bg = sqrt((2*W) / (rho*S))*(1./(4*C_D0.^2 +
C_D0.*pi*e*A*cos(phi)^2)).^(1/4); %True Air Speed, fps

%%Convert velocity from fps to kts using convvel. KTAS is true airspeed
in knots.
KTAS_bg = convvel(TAS_bg,'ft/s','kts');

%%Convert KTAS to KCAS using correctairspeed. KCAS is calibrated airspeed
in knots
%%Calibrated airspeed (CAS) is indicated airspeed corrected for
instrument and position error.
%%When flying at sea level under International Standard Atmosphere
conditions (15 °C, 1013 hPa, 0% humidity) calibrated airspeed is the same
as equivalent airspeed (EAS) and true airspeed (TAS).
KCAS_bg = correctairspeed(KTAS_bg,a,P,'TAS','CAS');

%%Calculate Best Glide Angle
%%If a glider is in a steady (constant velocity and no acceleration)
descent, it loses altitude as it travels. The flight path intersects the
ground at an angle called the glide angle.  
⑯
%%This is the angle between the flight path and the ground that provides
the highest L/D ratio.
gamma_bg_rad = asin( -sqrt((4.*C_D0')./(pi*e*A*cos(phi)^2 + 4.*C_D0')));

%%Convert glide angle from radians to degrees using convang
gamma_bg = convang(gamma_bg_rad,'rad','deg');

%%Calculate Best Glide Drag
%%Best glide drag can also be called as the point in the flight path at
which drag is minimum
D_bg = -W*sin(gamma_bg_rad);

%%Calculate Best Glide Lift
%%Best glide lift can also be called as the point in the flight path at
which lift is maximum
L_bg = W*cos(gamma_bg_rad);

%%Calculate Dynamic Pressure34 using dpressure
%%Dynamic pressure is the kinetic energy per unit volume of a fluid.
17Dynamic pressure is in fact one of the terms of Bernoulli's equation,
which can be derived from the conservation of energy for a fluid in
motion. In simplified cases, the dynamic pressure is equal to the
difference between the stagnation pressure and the static pressure
qbar = dpressure([TAS_bg' zeros(size(TAS_bg,2),2)], rho);

%%Calculate Drag and Lift Coefficients
%%Coefficient of drag at best glide is that coefficient of drag at which
drag is minimum
%%Coefficient of lift at best glide is that coefficient of lift at which
lift is maximum
C_D_bg = D_bg./ (qbar*S);
C_L_bg = L_bg./ (qbar*S);

%%Summary of Best Glide Values
disp(['Best True Air Speed in fps for gliding at ',num2str(h),' feet:
',num2str(TAS_bg)]);

```

```

disp(['Best True Air Speed in knots for gliding at ',num2str(h),' feet:
',num2str(KTAS_bg)]);
disp(['Best Calibrated Air Speed in knots for gliding at ',num2str(h),' feet:
',num2str(KCAS_bg)]);
disp(['Best Glide Angle in radians for gliding at ',num2str(h),' feet:
',num2str(gamma_bg_rad)]);
disp(['Best Glide Angle in degrees for gliding at ',num2str(h),' feet:
',num2str(gamma_bg)]);
disp(['Best value of drag in lbf for gliding at ',num2str(h),' feet:
',num2str(D_bg)]);
disp(['Best value of lift in lbf for gliding at ',num2str(h),' feet:
',num2str(L_bg)]);
disp(['Dynamic Pressure lb/ft^2 at ',num2str(h),' feet: ',num2str(qbar)]);
disp(['Best value of Drag Coefficient when gliding at ',num2str(h),' feet:
',num2str(C_D_bg)]);
disp(['Best value of Lift Coefficient when gliding at ',num2str(h),' feet:
',num2str(C_L_bg)]);

%%Set range of airspeeds and convert to KCAS using convvel and
correctairspeed:
TAS = (20:200)'; %True
airspeed, fps
KTAS = convvel(TAS,'ft/s','kts')'; %True airspeed,
kts
KCAS = correctairspeed(KTAS,a,P,'TAS','CAS')'; %Calibrated
airspeed, kts

%%Calculate Dynamic Pressure for new airspeeds using dpressure:
qbar = dpressure([TAS zeros(size(TAS,1),2)], rho); %lb/ft^2

%%Calculate parasite drag
%%Parasitic drag is drag that acts on an object when the object is
moving through a fluid. In the case of aerodynamic drag, the fluid is
the atmosphere.
%%Parasitic drag19 is a combination of form drag and skin friction drag.
Parasitic drag does not result from the generation of lift on the
object, and hence it is considered parasitic.
Dp = qbar*S.*C_D0; %lb.ft/s^2

%%Calculate induced drag
%%Induced drag is that part of the drag on an aerofoil which arises from
the development of lift.
Di = (2*W^2)/(rho*S*pi*e*A).* (TAS.^-2); %lb.ft/s^2

%%Calculate total drag
%%Total Drag produced by an aircraft is the sum of the Profile drag,
Induced drag, and Parasite drag. Total drag is primarily a function of
airspeed.
D = Dp + Di; %lb.ft/s^2

%%Approximate lift as weight (assuming small glide angle and small angle
of attack). At this speed, assuming
L = W;

%%Plot L/D versus KCAS
%%The maximum L/D occurs at approximately the best glide velocity
calculated above.
h1 = figure;
plot(KCAS,L./D);
title('Fig 27: L/D vs. KCAS');

```

```

xlabel('KCAS'); ylabel('L/D');
hold on
plot(KCAS_bg,L_bg/D_bg,'Marker','o','MarkerFaceColor','black','MarkerEdgeColor','black','Color','white');
hold off
legend('L/D','L_{bg}/D_{bg}','Location','Best');

%%Plot L/D versus TAS
h2 = figure;
plot(TAS,L./D);
title('Fig 28: L/D vs. TAS');
xlabel('TAS'); ylabel('L/D');
hold on
plot(TAS_bg,L_bg/D_bg,'Marker','o','MarkerFaceColor','black','MarkerEdgeColor','black','Color','white');
hold off
legend('L/D','L_{bg}/D_{bg}','Location','Best');

%%Plot L/D versus C_L
h3 = figure;
fplot(@(x) x/(C_D0+((x ^ 2)/(pi*e*A))),[0,5])
grid on

axis([0 1.306 0 12])
title('Fig 29: (L/D)_{max}')
xlabel('C_{L}')
ylabel('L/D')

%%Plot parasite, induced, and total drag curves
h4 = figure;
plot(KCAS,Dp,KCAS,Di,KCAS,D);
title('Fig 30: Parasite, induced, and total drag curves');
xlabel('KCAS'); ylabel('Drag, lbf');
hold on
plot(KCAS_bg,D_bg,'Marker','o','MarkerFaceColor','black','MarkerEdgeColor','black','Color','white');
hold off
legend('Parasite, D_p','Induced, D_i','Total, D','D_{bg}','Location','Best');

%%Plot the drag polar as C_D vs. C_L and clearly mark C_D_0 on the polar
h5 = figure;
fplot(@(x) C_D0+((x ^ 2)/(pi*e*A)),[-5,5])
grid on
title('Fig 31: Drag Polar')
xlabel('C_{L}')
ylabel('C_{D}')

%%Calculate Range and Endurance
%%Range is the maximum distance an aircraft can fly between take-off and landing, as limited by fuel capacity in powered aircraft, or cross-country speed and environmental conditions in unpowered aircraft.
%%Endurance is the maximum length of time that an aircraft can spend in cruising flight. In another word it is also the amount of an aircraft can stay on air with one load fuel
R = (L_bg/D_bg)*h; %Range in ft
hdot = ((-KCAS_bg).*(D_bg/W)); %Rate of Climb/Sink Rate
E = ((-h)/hdot); %Endurance/Time of Flight in seconds

```

```

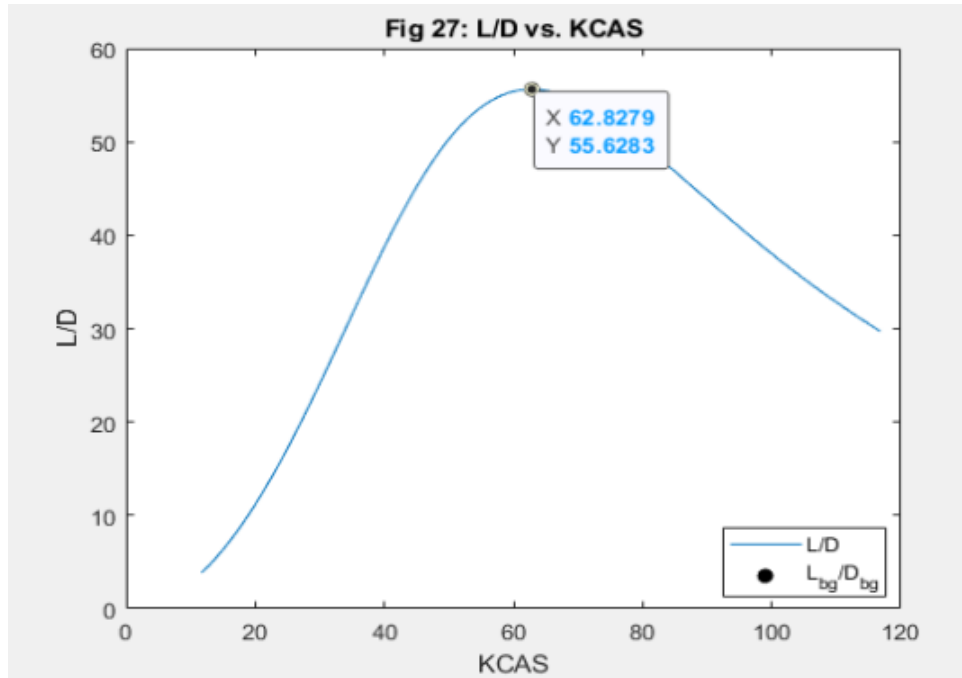
disp(['Best Glide Ratio at height of ',num2str(h),' feet:
',num2str(L_bg/D_bg)]);
disp(['Range of glider at height of ',num2str(h),' feet: ',num2str(R),' 
feet']);
disp(['Sink Rate of glider at height of ',num2str(h),' feet:
',num2str(hdot),' knots']);
disp(['Endurance of glider at height of ',num2str(h),' feet:
',num2str(E),' seconds']);

```

8.1.1 Output

Best True Air Speed in fps for gliding at 1000 feet: 107.5931
 Best True Air Speed in knots for gliding at 1000 feet: 63.7472
 Best Calibrated Air Speed in knots for gliding at 1000 feet: 62.8279
 Best Glide Angle in radians for gliding at 1000 feet: -0.017975
 Best Glide Angle in degrees for gliding at 1000 feet: -1.0299
 Best value of drag in lbf for gliding at 1000 feet: 23.7749
 Best value of lift in lbf for gliding at 1000 feet: 1322.5563
 Dynamic Pressure lb/ft² at 1000 feet: 13.3597
 Best value of Drag Coefficient when gliding at 1000 feet: 0.015812
 Best value of Lift Coefficient when gliding at 1000 feet: 0.87959
 Best Glide Ratio at height of 1000 feet: 55.6283
 Range of glider at height of 1000 feet: 55628.2709 feet
 Sink Rate of glider at height of 1000 feet: -1.1292 knots
 Endurance of glider at height of 1000 feet: 885.5502 seconds

8.1.2 Figures



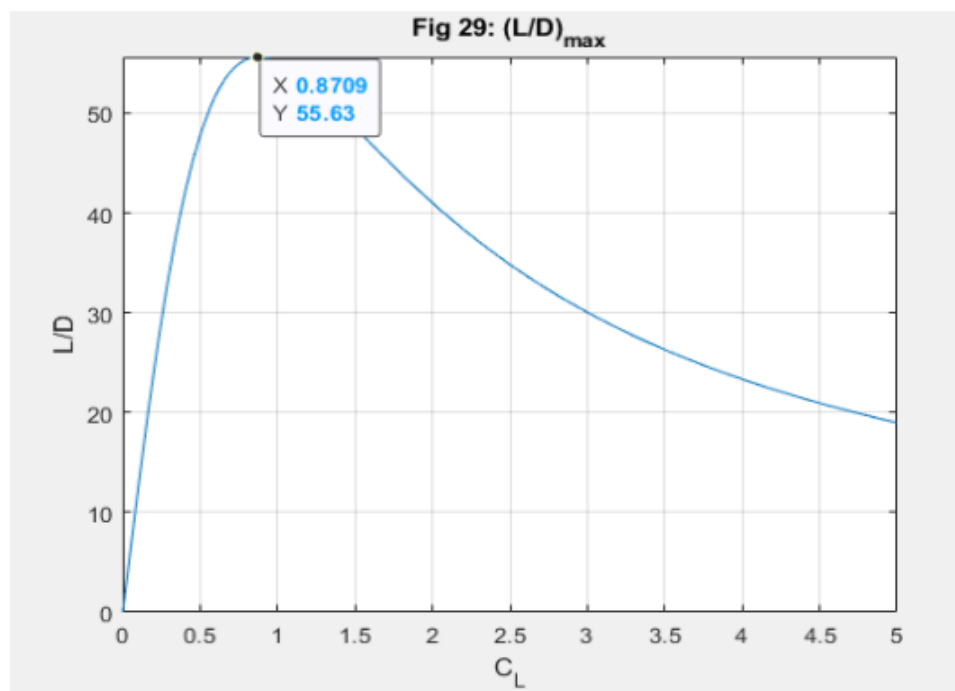
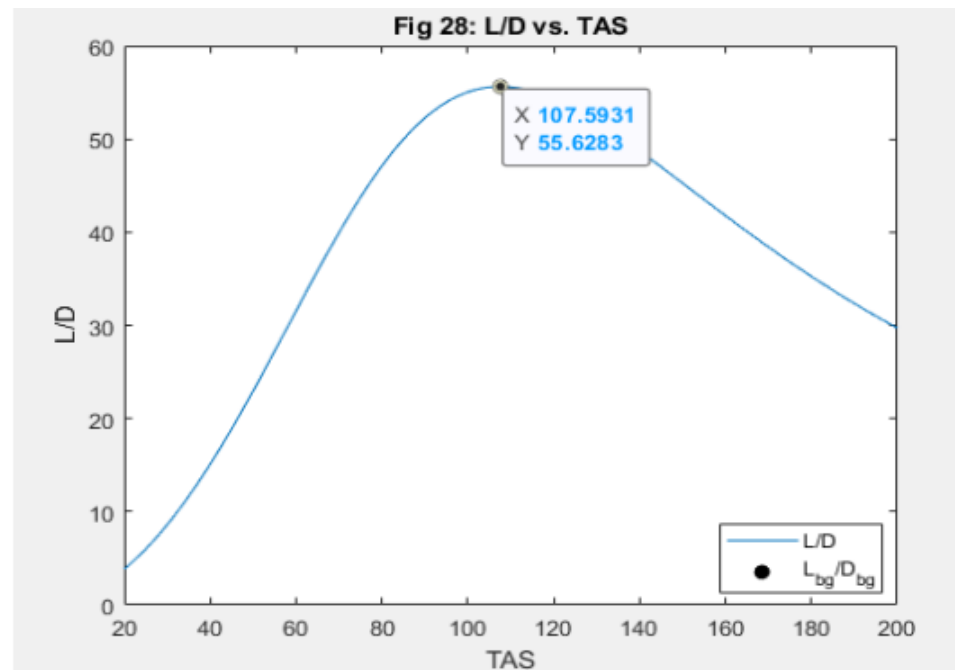


Fig 30: Parasite, induced, and total drag curves

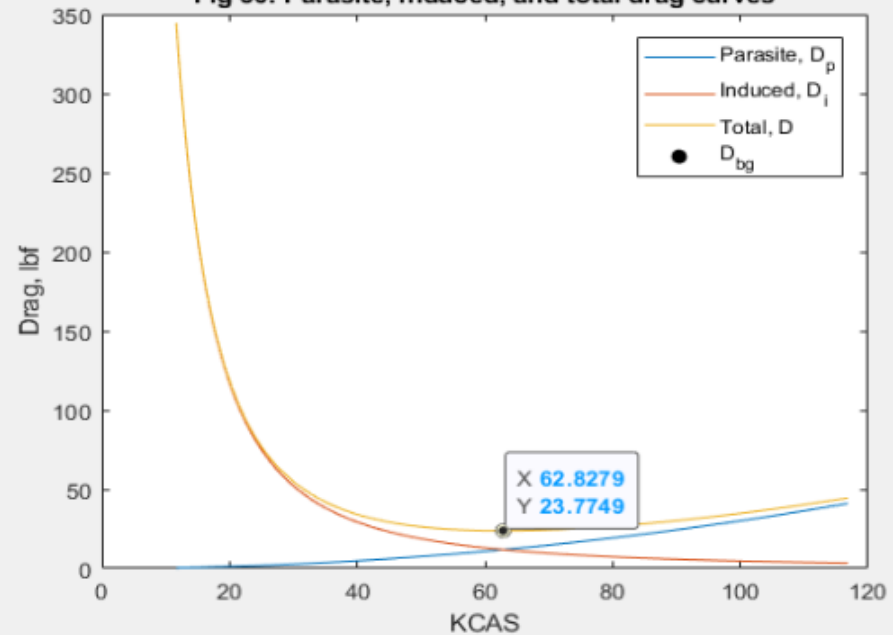
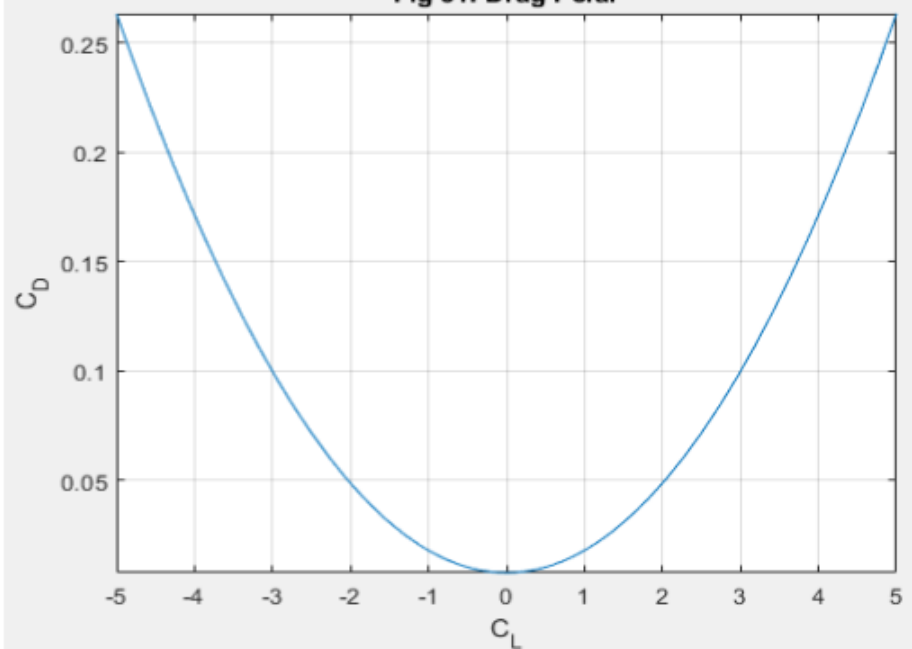


Fig 31: Drag Polar



9. ASW 22 BL Sailplane



Fig 32: ASW 22 BL Sailplane

ASW 22 BL

Span	m	(ft)	25	(82.02)	26.58	(87.20)
Wing area	m^2	(sqft)	16.31	(175.56)	16.688	(179.62)
Wing aspect ratio			38.32		42.336	
Wing airfoils			HQ 17 and DU 84-132/V3 at the wingtip			
Fuselage length	m	(ft)	8.1	(26.57)		
Cockpit height	m	(ft)	0.78	(2.55)		
Cockpit width	m	(ft)	0.64	(2.09)		
Height at tailplane	m	(ft)	1.66	(5.44)		
Empty mass	kg	(lb)	≈ 455	(1003)	≈ 465	(1025)
Max. take-off mass	kg	(lb)	750	(1653)		
Waterballast, max.	l	(lb)	235	(518)		
Useful load, max.	kg	(lb)	115	(253)		
Max. wing loading	kg/m^2	(lb/sqft)	46	(9.42)	45	(9.21)
Min. wing loading	kg/m^2	(lb/sqft)	32	(6.55)		
Max. speed	km/h	(kts)	280	(151)		
Min. sink	m/s	(ft/min)	≈ 0.41	(80.7)		
Best glide ratio (95 km/h)			60		62	

Fig 33: Technical Data of ASW 22 BL Sailplane

9.1 MATLAB Code Analysis (ASW 22 BL)

```
clc; clear; close all;

%%Given parameters of ASW-22BL sailplane
s = 87.20; %Wing Span, ft. The wingspan of a glider or an
airplane is the distance from one wingtip to the other wingtip.
S = 179.62; %Wing A17, ft2, The wing area is a projected area
of the planform bounded by leading and trailing edges and the wingtips
and is almost half of the total surface area.
A = 42.336; %Aspect Ratio, Aspect Ratio of a wing is defined to
be the square of the span divided by the wing area
l = 26.57; %Length, ft, It 33 the length of fuselage of a glider
H = 5.44; %Height, ft, It is the vertical distance from bottom
of the glider to the top of the glider
WSmax = 9.21; %Max wing loading, lbs/ft2, Total mass of an aircraft
divided by the area of its wingtip
WSmin = 6.55; %Min wing loading, lbs/ft2, Total mass of an aircraft
divided by the area of its wing root
Vs = 59.2374; %Stall Speed, ft/s, Stall speed is the slowest speed
an aircraft can fly to maintain level flight
Vmax = 255.176; %Max speed in rough air, ft/s, Max speed during cruise
flight
We = 1025; %Empty weight of glider, lbs
W = 1654; %Total weight of glider, lbs
C_D0 = 0.007906; %Parasite drag coefficient, Coefficient of parasitic
drag
e = 1; %Oswald Efficiency Factor, The Oswald efficiency,
similar to the span efficiency, is a correction factor that represents
the change in drag with lift 20 of a three-dimensional wing or airplane, as
compared with an ideal wing having the same aspect ratio and an
elliptical lift distribution.
Clmax = 1.7; %Max lift coefficient
Clmin = -0.1; %Min lift coefficient

%%Set the current conditions for sailplane
h = 1000; %Altitude, ft, It is the vertical distance of the
sailplane above the terrain over which it is flying
phi = 0; %Bank Angle, deg, The bank angle is the angle at
which the vehicle is inclined 9 about its longitudinal axis with respect to
the horizontal.

%%Convert altitude to meters using convlength
h_m = convlength(h,'ft','m');

%%Calculate atmospheric parameters based on altitude using atmoscoesa
[T, a, P, rho] = atmoscoesa(h_m, 'Error'); %These values are absolute
temperature, speed of sound for the input geopotential altitude,
pressure, and density.

%%Convert density from metric to English units using convdensity
rho = convdensity(rho,'kg/m^3','slug/ft^3');

%%Calculate Best Glide Data
%%The true airspeed (TAS; also KTAS, for knots true airspeed) of an
aircraft is the speed of the aircraft relative to the airmass in which
it is flying.
TAS_bg = sqrt((2*W) / (rho*S))*(1./(4*C_D0.^2 +
C_D0.*pi*e*A*cos(phi).^2)).^(1/4); %True Air Speed, fps
```

```

%%Convert velocity from fps to kts using convvel. KTAS is true airspeed
in knots.
KTAS_bg = convvel(TAS_bg,'ft/s','kts');

%%Convert KTAS to KCAS using correctairspeed. KCAS is calibrated airspeed
in knots
%%Calibrated airspeed (CAS) is indicated airspeed corrected for
instrument and position error.
%%When flying at sea level under International Standard Atmosphere
conditions (15 °C, 1013 hPa, 0% humidity) calibrated airspeed is the same
as equivalent airspeed (EAS) and true airspeed (TAS).
KCAS_bg = correctairspeed(KTAS_bg,a,P,'TAS','CAS');

%%Calculate Best Glide Angle
%%If a glider is in a steady (constant velocity and no acceleration)
descent, it loses altitude as it travels. The flight path intersects the
ground at an angle called the glide angle.
13 %%This is the angle between the flight path and the ground that provides
the highest L/D ratio.
gamma_bg_rad = asin( -sqrt((4.*C_D0')./(pi*e*A*cos(phi)^2 + 4.*C_D0')) ) ;

%%Convert glide angle from radians to degrees using convang
gamma_bg = convang(gamma_bg_rad,'rad','deg');

%%Calculate Best Glide Drag
%%Best glide drag can also be called as the point in the flight path at
which drag is minimum
D_bg = -W*sin(gamma_bg_rad);

%%Calculate Best Glide Lift
%%Best glide lift can also be called as the point in the flight path at
which lift is maximum
L_bg = W*cos(gamma_bg_rad);

%%Calculate Dynamic Pressure34 using dpressure
%%Dynamic pressure is the kinetic energy per unit volume of a fluid.
17 %%Dynamic pressure is in fact one of the terms of Bernoulli's equation,
%%which can be derived from the conservation of energy for a fluid in
%%motion. In simplified cases, the dynamic pressure is equal to the
%%difference between the stagnation pressure and the static pressure
qbar = dpressure([TAS_bg' zeros(size(TAS_bg,2),2)], rho);

%%Calculate Drag and Lift Coefficients
%%Coefficient of drag at best glide is that coefficient of drag at which
drag is minimum
%%Coefficient of lift at best glide is that coefficient of lift at which
lift is maximum
C_D_bg = D_bg./ (qbar*S);
C_L_bg = L_bg./ (qbar*S);

%%Summary of Best Glide Values
disp(['Best True Air Speed in fps for gliding at ',num2str(h),' feet:
',num2str(TAS_bg)]);
disp(['Best True Air Speed in knots for gliding at ',num2str(h),' feet:
',num2str(KTAS_bg)]);
disp(['Best Calibrated Air Speed in knots for gliding at ',num2str(h),' feet:
',num2str(KCAS_bg)]);

```

```

disp(['Best Glide Angle in radians for gliding at ',num2str(h),' feet:
',num2str(gamma_bg_rad)]);
disp(['Best Glide Angle in degrees for gliding at ',num2str(h),' feet:
',num2str(gamma_bg)]);
disp(['Best value of drag in lbf for gliding at ',num2str(h),' feet:
',num2str(D_bg)]);
disp(['Best value of lift in lbf for gliding at ',num2str(h),' feet:
',num2str(L_bg)]);
disp(['Dynamic Pressure lb/ft^2 at ',num2str(h),' feet: ',num2str(qbar)]);
disp(['Best value of Drag Coefficient when gliding at ',num2str(h),' feet:
',num2str(C_D_bg)]);
disp(['Best value of Lift Coefficient when gliding at ',num2str(h),' feet:
',num2str(C_L_bg)]);

%%Set range of airspeeds and convert to KCAS using convvel and
correctairspeed:
TAS = (20:200)'; %True
airspeed, fps
KTAS = convvel(TAS,'ft/s','kts'); %True airspeed,
kts
KCAS = correctairspeed(KTAS,a,P,'TAS','CAS'); %Calibrated
airspeed, kts

%%Calculate Dynamic Pressure for new airspeeds using dpressure:
qbar = dpressure([TAS zeros(size(TAS,1),2)], rho); %lb/ft^2

%%Calculate parasite drag
%%Parasitic drag is drag that acts on an object when the object is
moving through a fluid. In the case of aerodynamic drag, the fluid is
the atmosphere.
%%Parasitic drag 19 is a combination of form drag and skin friction drag.
Parasitic drag does not result from the generation of lift on the
object, and hence it is considered parasitic.
Dp = qbar*S.*C_D0; %lb.ft/s^2

%%Calculate induced drag
%%Induced drag is that part of the drag on an aerofoil which arises from
the development of lift.
Di = (2*W^2)/(rho*pi*e*A).* (TAS.^-2); %lb.ft/s^2

%%Calculate total drag
%%Total Drag produced by an aircraft is the sum of the Profile drag,
Induced drag, and Parasite drag. Total drag is primarily a function of
airspeed.
D = Dp + Di; %lb.ft/s^2

%%Approximate lift as weight (assuming small glide angle and small angle
of attack). At this speed, assuming
L = W;

%%Plot L/D versus KCAS
%%The maximum L/D occurs at approximately the best glide velocity
calculated above.
h1 = figure;
plot(KCAS,L./D);
title('Fig 34: L/D vs. KCAS');
xlabel('KCAS'); ylabel('L/D');
hold on
plot(KCAS_bg,L_bg/D_bg,'Marker','o','MarkerFaceColor','black','MarkerEdgeColor','black','Color','white');

```

```

hold off
legend('L/D','L_{bg}/D_{bg}','Location','Best');

%%Plot L/D versus TAS
h2 = figure;
plot(TAS,L./D);
title('Fig 35: L/D vs. TAS');
xlabel('TAS'); ylabel('L/D');
hold on
plot(TAS_bg,L_bg/D_bg,'Marker','o','MarkerFaceColor','black','MarkerEdgeColor','black','Color','white');
hold off
legend('L/D','L_{bg}/D_{bg}','Location','Best');

%%Plot L/D versus C_L
h3 = figure;
fplot(@(x) x/(C_D0+((x ^ 2)/(pi*e*A))),[0,5])
grid on

axis([0 1.306 0 12])
title('Fig 36: (L/D)_{max}')
xlabel('C_{L}')
ylabel('L/D')

%%Plot parasite, induced, and total drag curves
h4 = figure;
plot(KCAS,Dp,KCAS,Di,KCAS,D);
title(' Fig 37: Parasite, induced, and total drag curves');
xlabel('KCAS'); ylabel('Drag, lbf');
hold on
plot(KCAS_bg,D_bg,'Marker','o','MarkerFaceColor','black','MarkerEdgeColor','black','Color','white');
hold off
legend('Parasite, D_p','Induced, D_i','Total,
D','D_{bg}','Location','Best');

%%Plot the drag polar as C_D vs. C_L and clearly mark C_D_0 on the polar
h5 = figure;
fplot(@(x) C_D0+((x ^ 2)/(pi*e*A)),[-5,5])
grid on
title('Fig 38: Drag Polar')
xlabel('C_{L}')
ylabel('C_{D}')
format long

%%Calculate Range and Endurance
%%Range is the maximum distance an aircraft can fly between take-off and landing, as limited by fuel capacity in powered aircraft, or cross-country speed and environmental conditions in unpowered aircraft.
%%Endurance is the maximum length of time that an aircraft can spend in cruising flight. In another word it is also the amount of an aircraft can stay on air with one load fuel
R = (L_bg/D_bg)*h; %Range in ft
hdot = ((-KCAS_bg).* (D_bg/W)); %Rate of Climb/Sink Rate
E = ((-h)/hdot); %Endurance/Time of Flight in seconds

R1 = (64.85)*h; %Range in ft
hdot1 = ((-59.4).* (D_bg/W)); %Rate of Climb/Sink Rate
E1 = ((-h)/hdot1); %Endurance/Time of Flight in seconds

```

```

disp(['Best Glide Ratio at height of ',num2str(h),' feet:
',num2str(L_bg/D_bg)]);
disp(['Range of glider at height of ',num2str(h),' feet: ',num2str(R),' 
feet']);
disp(['Sink Rate of glider at height of ',num2str(h),' feet:
',num2str(hdot),' knots']);
disp(['Endurance of glider at height of ',num2str(h),' feet:
',num2str(E),' seconds']);
disp(['Actual Range: ',num2str(R1),' feet']);
disp(['Actual Sink Rate: ',num2str(hdot1),' knots']);
disp(['Actual Endurance: ',num2str(E),' seconds']);

```

9.1.1 Output

Best True Air Speed in fps for gliding at 1000 feet: 88.2057
 Best True Air Speed in knots for gliding at 1000 feet: 52.2605
 Best Calibrated Air Speed in knots for gliding at 1000 feet: 51.5042
 Best Glide Angle in radians for gliding at 1000 feet: -0.015419
 Best Glide Angle in degrees for gliding at 1000 feet: -0.88342
 Best value of drag in lbf for gliding at 1000 feet: 25.5013
 Best value of lift in lbf for gliding at 1000 feet: 1653.8034
 Dynamic Pressure lb/ft² at 1000 feet: 8.9789
 Best value of Drag Coefficient when gliding at 1000 feet: 0.015812
 Best value of Lift Coefficient when gliding at 1000 feet: 1.0254
 Best Glide Ratio at height of 1000 feet: 64.8517
 Range of glider at height of 1000 feet: 64851.7122 feet
 Sink Rate of glider at height of 1000 feet: -0.79409 knots
 Endurance of glider at height of 1000 feet: 1259.3028seconds
 Actual Range: 64850 feet
 Actual Sink Rate: -0.91583 knots
 Actual Endurance: 1259.3028 seconds

9.1.2 Figures

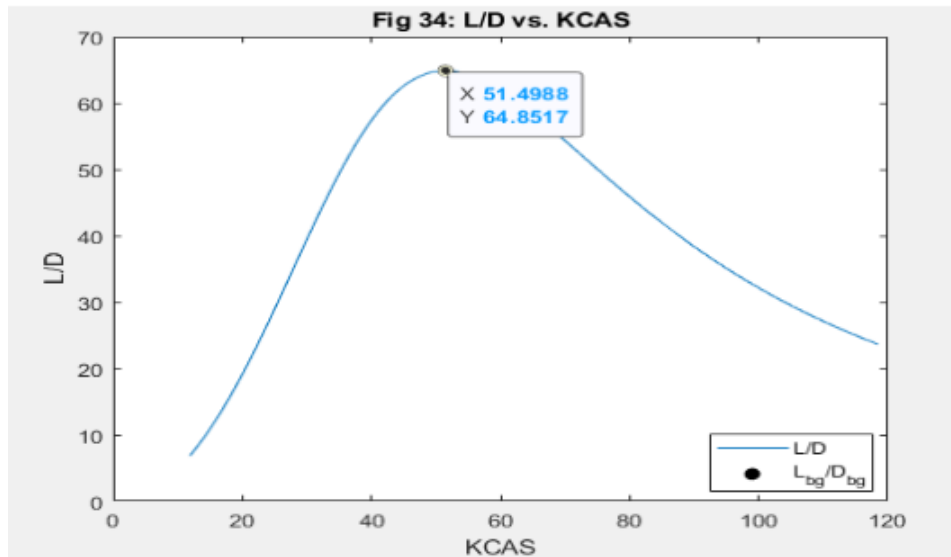


Fig 35: L/D vs. TAS

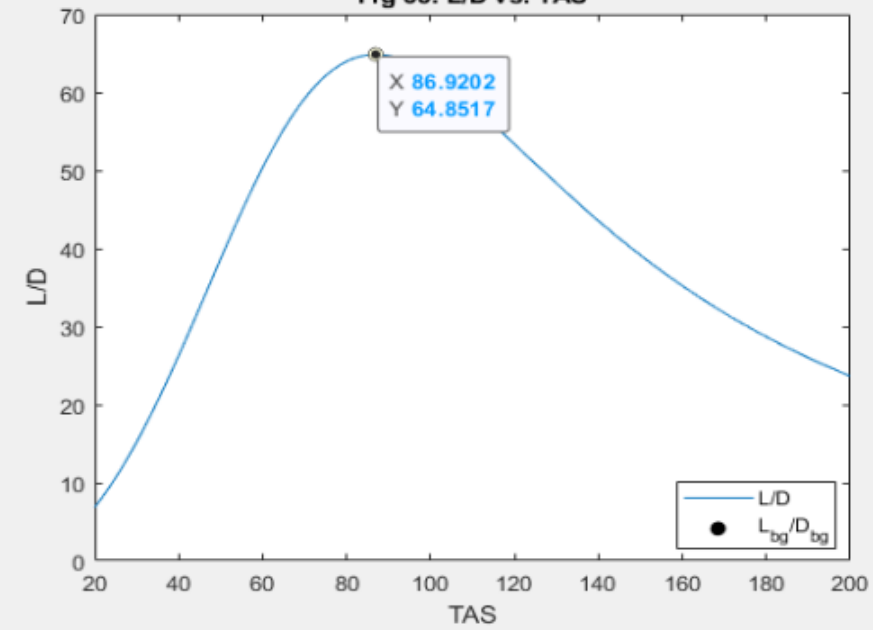


Fig 36: $(L/D)_{max}$

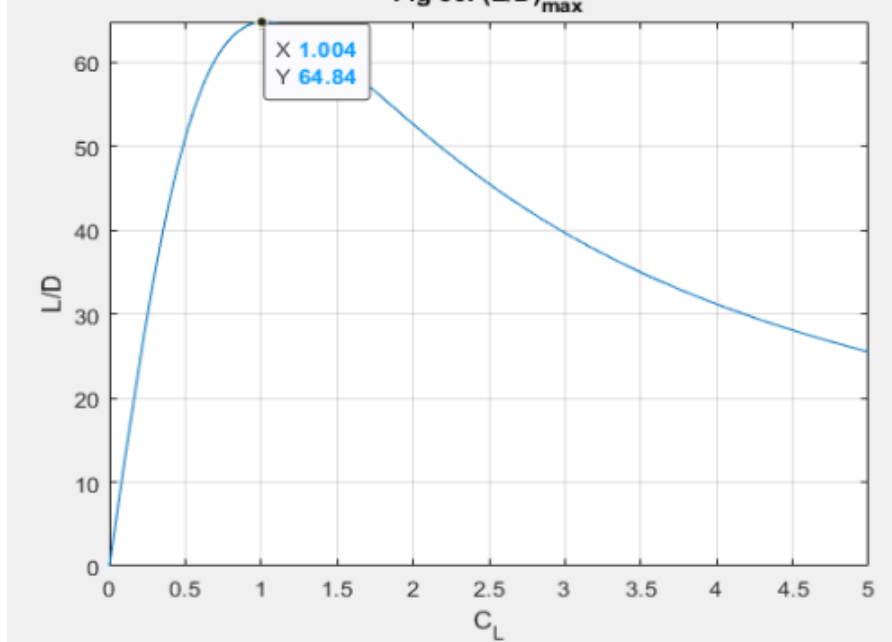


Fig 37: Parasite, induced, and total drag curves

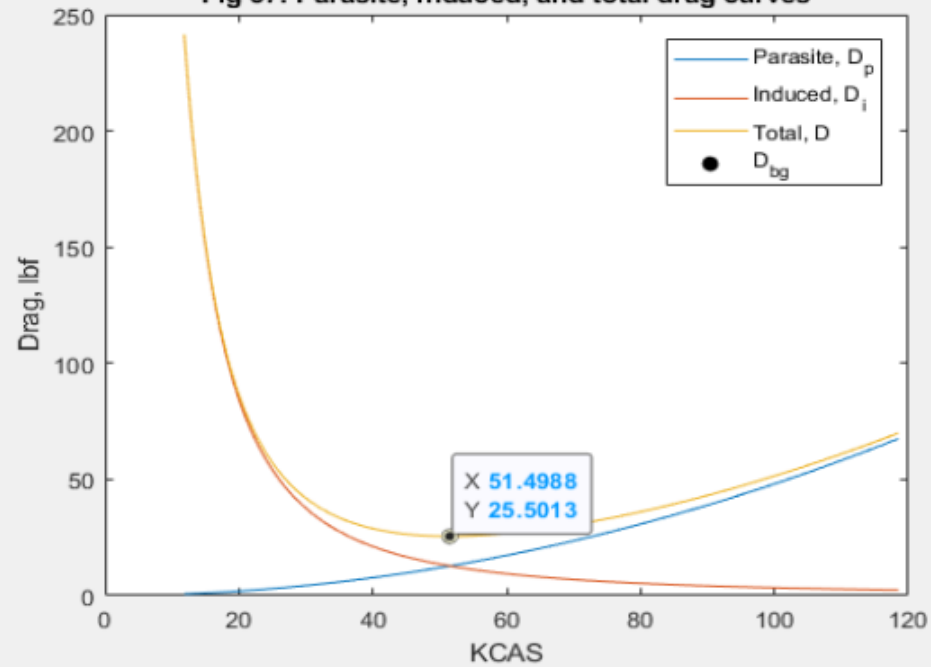
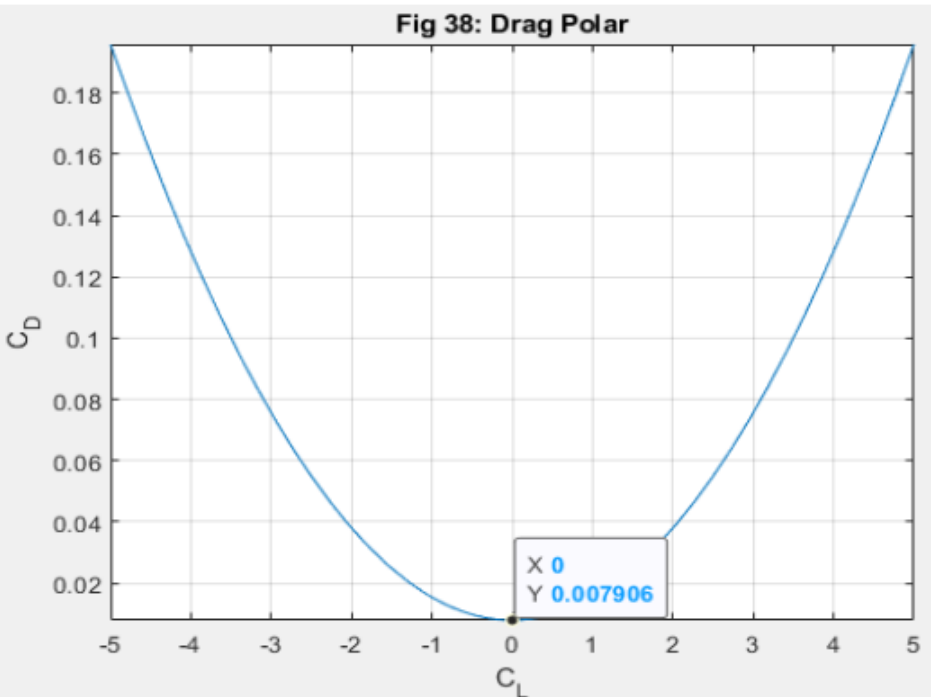


Fig 38: Drag Polar



10. Verification of MATLAB Results

To verify the above results, we will use the actual configuration aerodynamics data of the ASW 22 BL sailplane which is provided by the manufacturing company of this sailplane. From the configuration data, following speed polar and observations of the sailplane are taken for verification purposes.

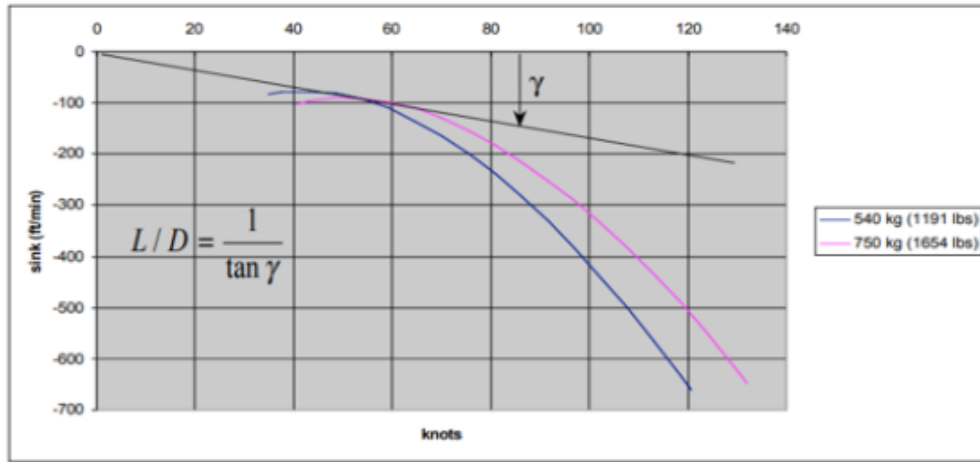


Fig 39: ASW 22 BL Factory Speed Polar

Observations:

Min. sink: 79 fpm @ 43.2 KCAS (1191 lbs. / CL = 1.05)

Best glide: 64.85 @ 59.4 KCAS (1654 lbs. / CL = 0.77)

Max Speed: 151 KCAS

Stall Speed: 35.3 KCAS (light A/C)

41.5 KCAS (heavy A/C)

(Flaps 9° / CLmax = 1.58)

Now, let's compare the results:

Table 2: Comparison of MATLAB Results and Glider Manual Results

Parameters	MATLAB Results	Glider Manual Results
Glide Ratio	64.8517	64.8500
Best C _l	1.0254	0.77
Best CAS (knots)	51.5042	59.4
Min. Sink Rate (knots)	0.79409	0.91583
Range (at altitude of 1000fts) (fts)	64851.7122	64849.9999
Endurance (at altitude of 1000fts) (s)	1259.3028	1091.9095

10.1 Analysis

ASW 22 BL:

Glide Ratio is almost perfectly matched. A difference in C_l value can be seen. This shows the difference between calculated and observed values of C_l . It happened because our calculations assumed steady atmospheric conditions which, in real case, is extremely rare when we consider sailplanes because a sailplane almost never flies in steady atmosphere. If a sailplane were to fly in steady atmosphere, it will quickly lose its altitude because of the lack of an engine. So, to compensate for the lower value of C_l , pilots deploy flaps. These flaps recover that lost C_l value and hence the glide ratio is maintained. It can be seen from the observations in the configuration data, that max value of C_l is achieved by flap deflection of 9°.

Next parameter is best Calibrated Airspeed (CAS). Numerical calculations produce somewhat lower value of CAS than actual best CAS. This is the direct application of the local increase in lift. The forward force acting on the glider includes the horizontal component of lift coefficient. So, if the C_l increases locally, CAS will also increase.

From the speed polar, we can find the corresponding value of min. sink rate. Alternatively, we can also find it by the formula used in MATLAB Coding which is what we used to determine it. We can easily observe that both results are same. So, we got higher value of min. sink rate through glider manual because of the higher value of CAS.

To understand this, one must know the relation between Glide Ratio, CAS, and Min. Sink rate.

Relation between glide ratio, CAS and min. sink rate

The glide ratio at a particular airspeed can be estimated from the glide polar using:

$$\text{Glide Ratio} \approx \frac{\text{CAS}}{\text{Min. Sink Rate}} : 1$$

This means that Glide Ratio is simply the slope of the tangent drawn to the speed polar of the sailplane provided that both of these parameters are in the same units.

Hence, for the same value of glide ratio, if value of CAS is higher (as in the configuration data), min. sink rate will also be higher which is what we observe in the comparison table above. Range and Endurance are calculated for the altitude of 1000 fts. Range is almost equal because it is directly dependent on the glide ratio. Numerical results produced higher value of endurance because it is inversely dependent on min. sink rate which is better because Endurance depicts the time for which the aircraft can fly.

Diana 3:

As for the Diana 3 sailplane, it is a very modern sailplane with several tests still needed to be done. So, we cannot really verify those results. But we have used exactly same numerical method in case of Diana 3 also. Max value of glide ratio observed in the Diana 3 is 54 at 66.9546 knots while we achieved a value larger than 54 at speed lower than the observed one (Glide Ratio of 55.6283 @ CAS 62.8279). This alone can validate our numerical results.

11. Ansys Simulations

We will now do the turbulence testing for the aerofoil which is used in ASW 22 BL sailplane: DU84-132/V3. Modern sailplanes deploy the use of variable aerofoil for the wing cross section to optimize performance. So, this aerofoil is used on the wingtip.

For our turbulence model, we will use the Reynolds number (Re) of 1,000,000 because for Re must be greater than 500,000 for turbulent flow. Also, we will use the values of density of air and dynamic viscosity at 2000 fts of altitude above sea level in this testing. We will then verify our results by comparing our results with the aerofoil database available on www.aerofoiltools.com.

11.1 Steps

1. Firstly, we need an aerofoil coordinates file which can be downloaded from the above website and then modify its format to be able to import it successfully in the design modeler.
2. After we have the coordinates file, a curve is need to be created from those coordinates and generate the surface from those curves.
3. We will then modify its dimensions by setting the scale from body transformation and set it according to the required chord length.
4. We now need a fluid flow region around this aerofoil and the dimensions of this region must be at least 10 times the chord length of aerofoil. Suppose the chord is of 1m, then fluid flow region should be at least 10m. on each side of the aerofoil. Practice shows that shape of this fluid flow region should be C-shape in front of the aerofoil.
5. We then use Boolean feature to subtract the surface of aerofoil from the fluid flow region and then freeze the geometry and supress the line body of aerofoil.
6. We will then move on to the meshing phase. To mesh this geometry, add a bunch of edge sizing and use the face meshing because a face meshing is very fast if computational power is limited.
7. Although, we will have to divide the geometry in design modeler first into six faces to have accurate meshing.
8. We now have to create named selections. The C-shaped surface in front of the aerofoil and horizontal surface around the aerofoil can all be named Inlet whereas the surface behind the aerofoil will be Outlet and lastly the lines of the aerofoil will be named Aerofoil.
9. Coming to the setup, we just need to select parallel processing for faster computation. Double precision is not needed in this case.
10. Firstly, we need to choose model. Go to Models > Viscous > Spalart Allmaras > Strain/Vorticity Based > Curvature Correction > OK.
11. Next, go to Materials > Fluid > Air > Change the density and viscosity according to the altitude requirements > Change/Create > Close.
12. Now, we have to set up boundary conditions. Boundary Conditions > Inlet > inlet (velocity-inlet). Choose Magnitude and Direction in Velocity Specification Method. Put the Velocity Magnitude after calculating it with the formula $V = \frac{Re \cdot \mu}{\rho \cdot c}$ where c is the chord length, ρ is density and μ is dynamic viscosity. Change the Turbulent Viscosity ratio to 1 to converge results faster > OK.
13. Come to Reference Values > Compute from > Inlet.
14. Move to Methods under Solutions > Momentum > Second Order Upwind > Modified Turbulent Viscosity > Second Order Upwind.

15. Report Definitions > New > Force Reports > Drag > Report Output Type: Drag Coefficient > Select aerofoil in Wall > Create > Report File > Report Plot > Frequency > 10 > Print to Console > OK > Close.
16. Repeat Step 15 for Lift Coefficient Report also.
17. We can repeat the previous step if we want reports of Lift and Drag forces instead of coefficients.
18. Initialization > Hybrid Initialization > Initialize.
19. Run Calculation > Number of Iterations: 5000 > Reporting Interval: 10 > profile Update Interval: 10 > Calculate.
20. After the plots are converged, we can stop the calculation and generate contours and compute values of C_l and C_d .

11.2 Results

Static Pressure Contour:

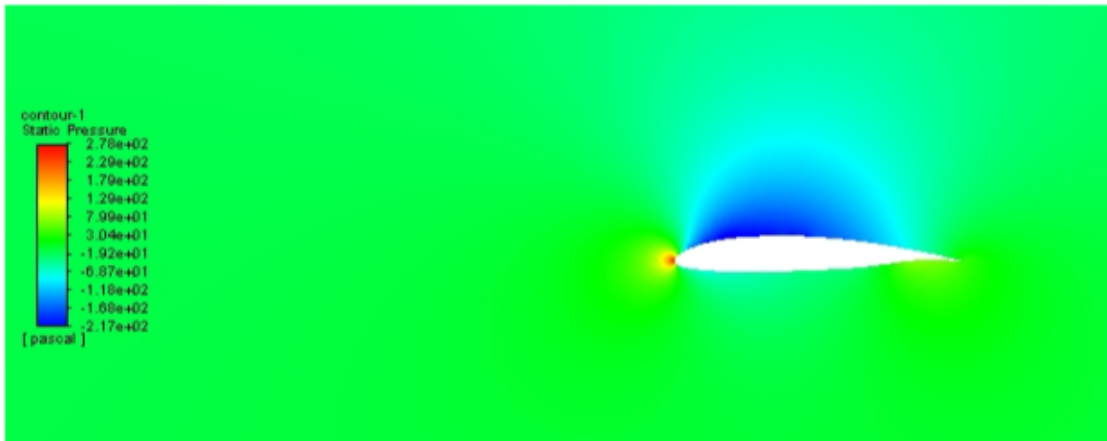


Fig 40: Static pressure contour at $\alpha = 0^\circ$

Velocity Contour:

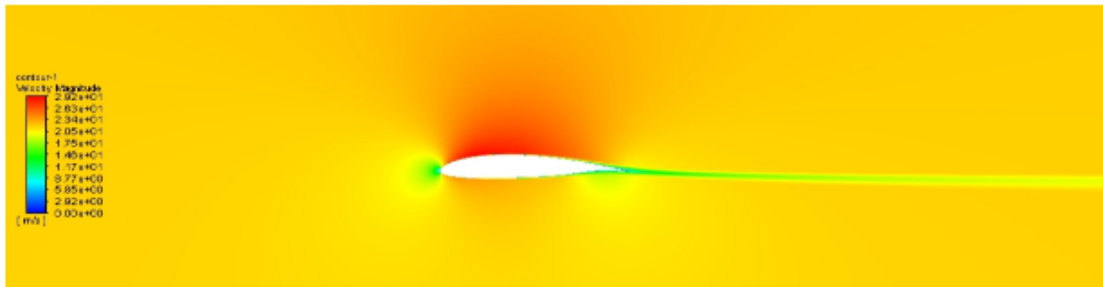


Fig 41: Velocity contour at $\alpha = 0^\circ$

Value of $C_l = 0.29730332$

Value of $C_d = 0.008094392$

These values are pretty accurate. However, for verification purposes, we need these values of C_L and C_d at different values of angle of attack (AoA).

To obtain these values, we will simply change X and Y components of flow direction according to the AoA while specifying the boundary conditions at inlet. For ex: if I need to run calculations at AoA of 3° , then in the X-Component of flow direction I will write 0.998629535 ($\cos(\text{AoA})$) instead of 1 and in Y-Component of flow direction I will write 0.052335956 ($\sin(\text{AoA})$) instead of 0. After updating the boundary conditions, we also have to change the definitions of lift and drag coefficients in the report definitions section according to the aerodynamics equations.

$$L = F_y \cdot \cos(\alpha) - F_x \cdot \sin(\alpha)$$

$$D = F_x \cdot \cos(\alpha) + F_y \cdot \sin(\alpha)$$

So, under the Force Vectors of Lift Coefficient, we will write values of ' $-\sin(\alpha)$ ' and ' $\cos(\alpha)$ ' in the X and Y columns respectively.

Similarly, for Drag Coefficient, we will write values of ' $\cos(\alpha)$ ' and ' $\sin(\alpha)$ ' in the X and Y columns respectively.

After this, we simply have to reinitialize and run calculations until the plots converge.

Contours of static pressure and velocity for different values of α are given below:

Contours at $\alpha = -12^\circ$:

Static Pressure:

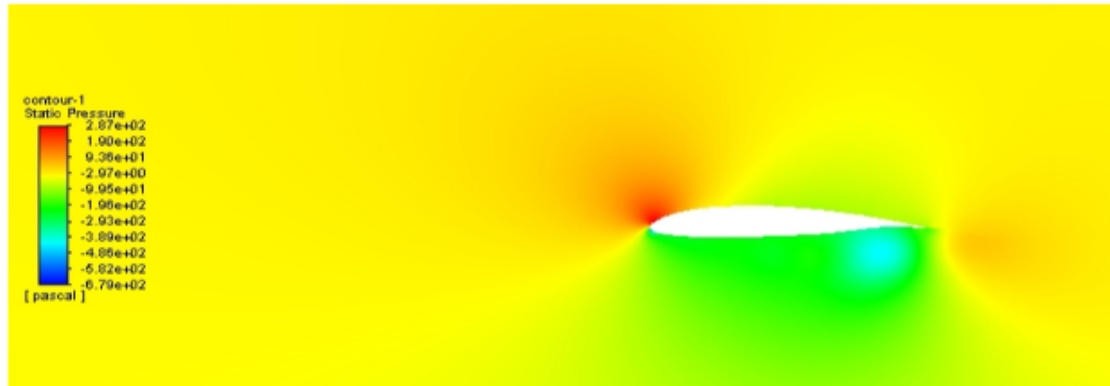


Fig 42: Static pressure contour at $\alpha = -12^\circ$

Velocity:

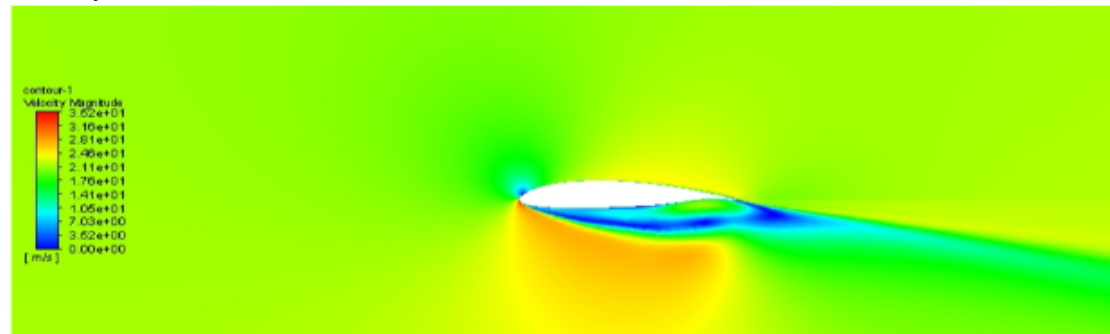


Fig 43: Velocity contour at $\alpha = -12^\circ$

Contours at $\alpha = -9^\circ$:

Static Pressure:

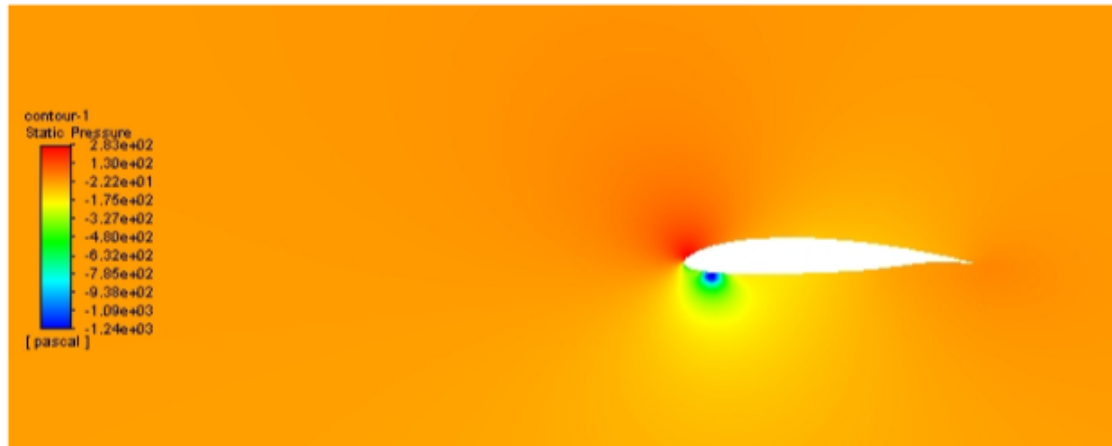


Fig 44: Static pressure contour at $\alpha = -9^\circ$

Velocity:

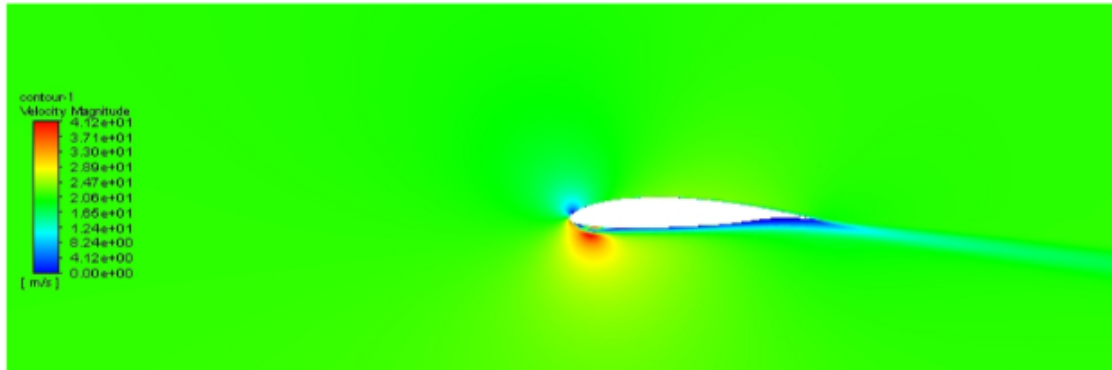


Fig 45: Velocity contour at $\alpha = -9^\circ$

Contours at $\alpha = -6^\circ$:

Static Pressure:

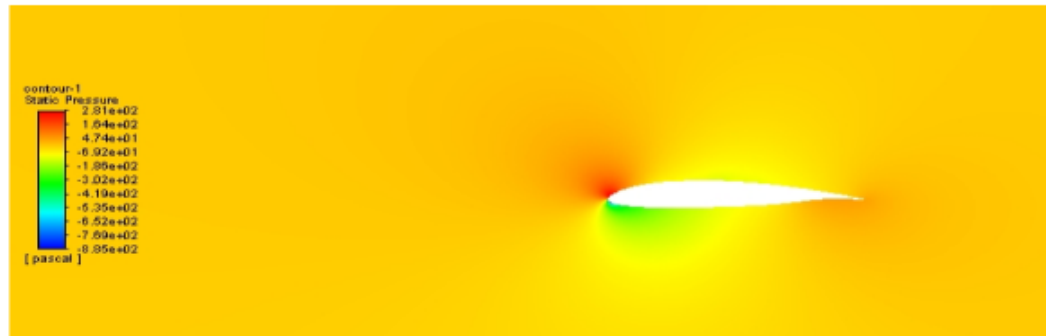


Fig 46: Static pressure contour at $\alpha = -6^\circ$

Velocity:

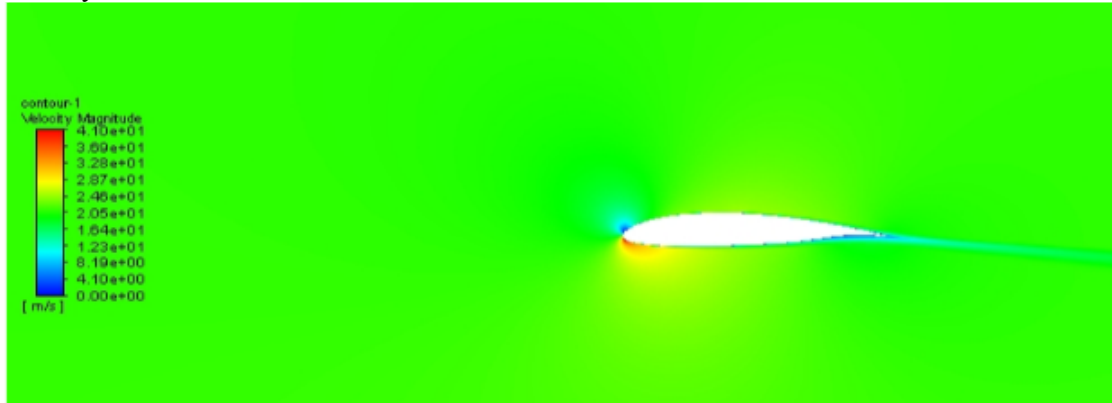


Fig 47: Velocity contour at $\alpha = -6^\circ$

Contours at $\alpha = -3^\circ$:

Static Pressure:

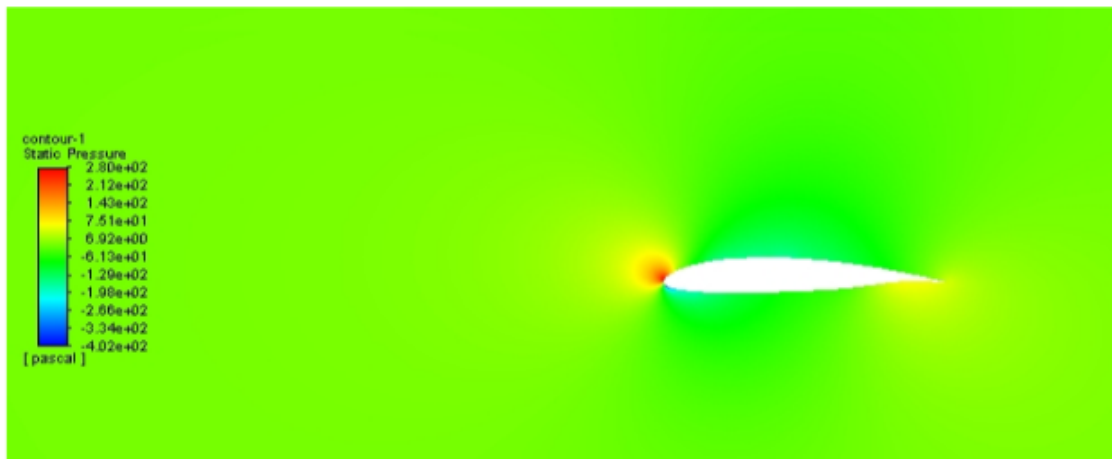


Fig 48: Static pressure contour at $\alpha = -3^\circ$

Velocity:

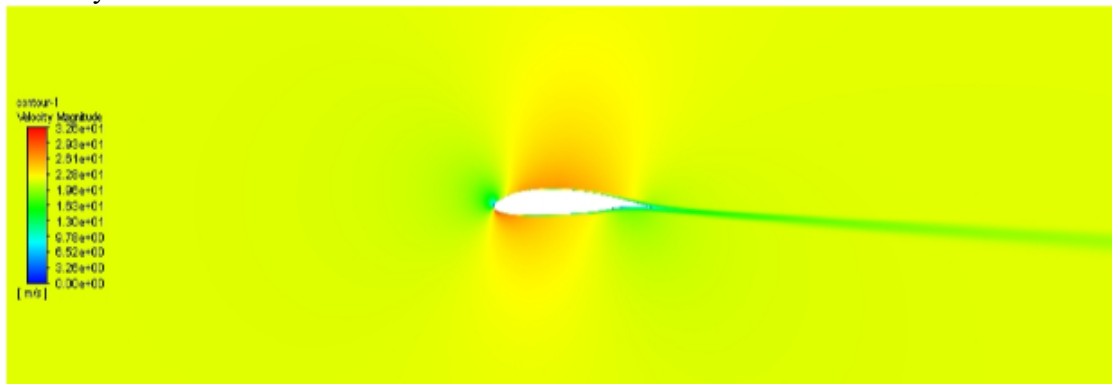


Fig 49: Velocity contour at $\alpha = -3^\circ$

Contours at $\alpha = 3^\circ$:

Static Pressure:

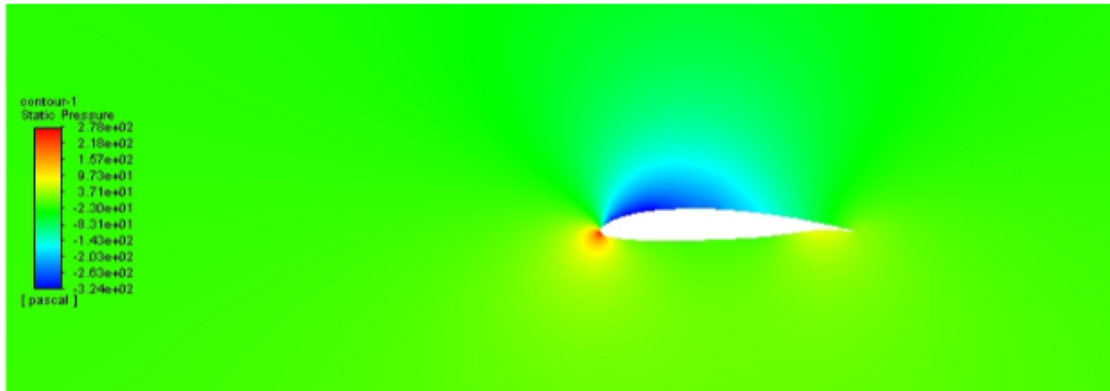


Fig 50: Static pressure contour at $\alpha = 3^\circ$

Velocity:

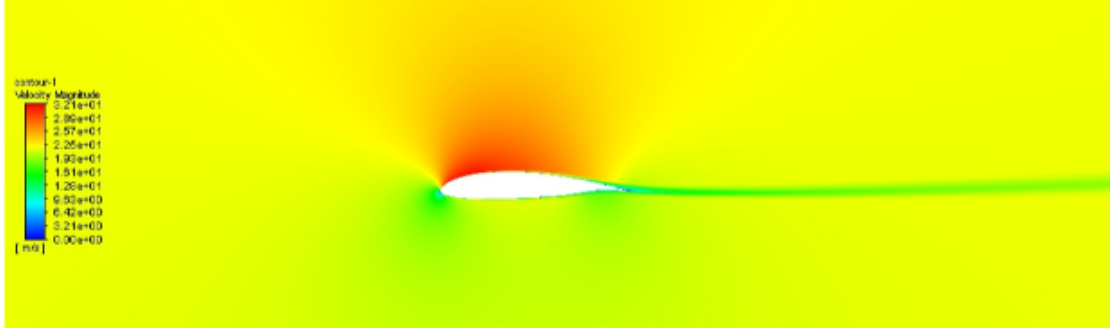


Fig 51: Velocity contour at $\alpha = 3^\circ$

Contours at $\alpha = 9^\circ$:

Static Pressure:

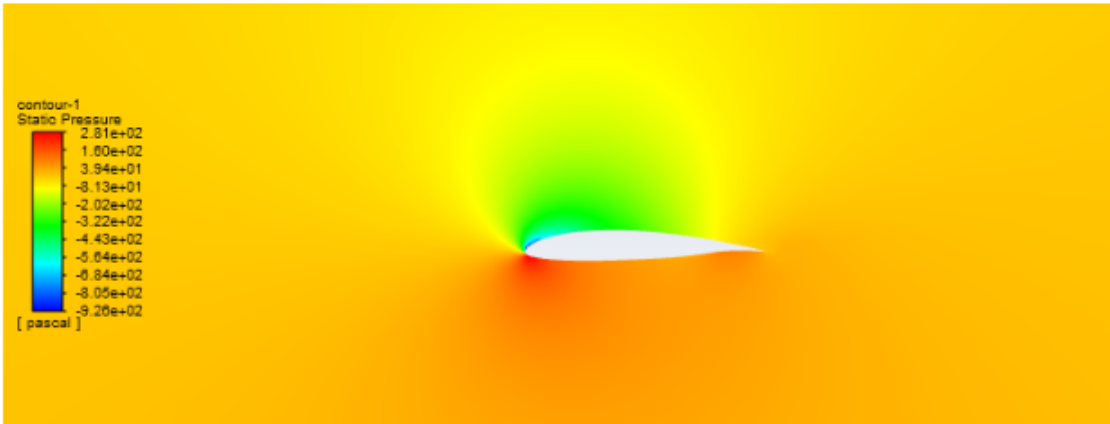


Fig 52: Static pressure contour at $\alpha = 9^\circ$

Velocity:

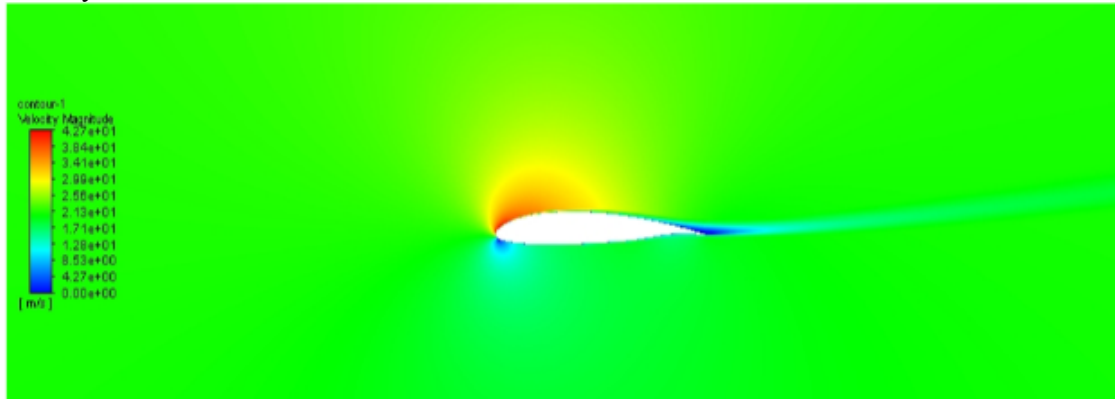


Fig 53: Velocity contour at $\alpha = 9^\circ$

Contours at $\alpha = 15^\circ$:

Static Pressure:

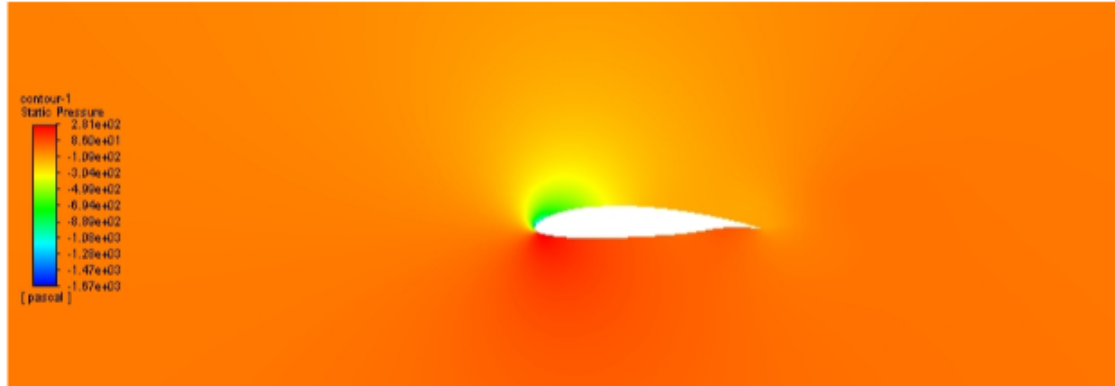


Fig 54: Static pressure contour at $\alpha = 15^\circ$

Velocity:

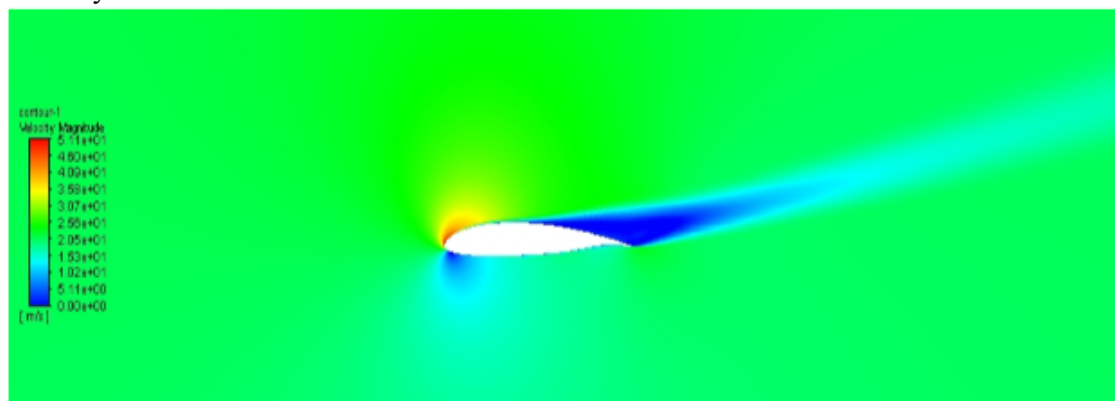


Fig 55: Velocity contour at $\alpha = 15^\circ$

Contours at $\alpha = 18^\circ$:

Static Pressure:

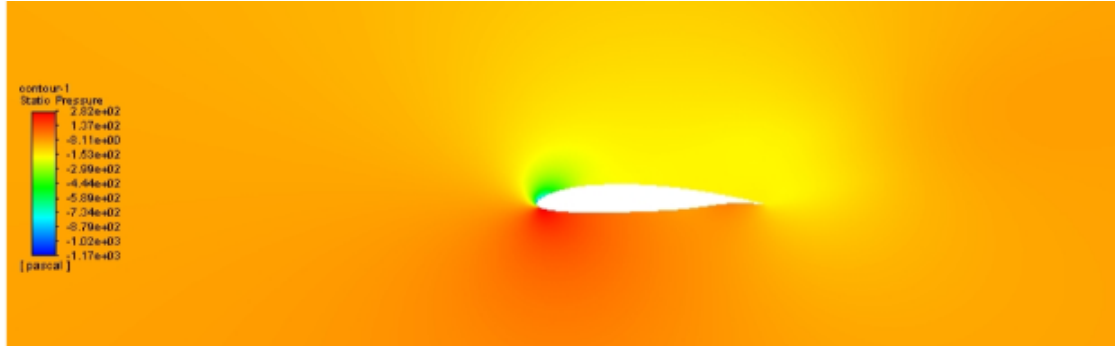


Fig 56: Static pressure contour at $\alpha = 18^\circ$

Velocity:

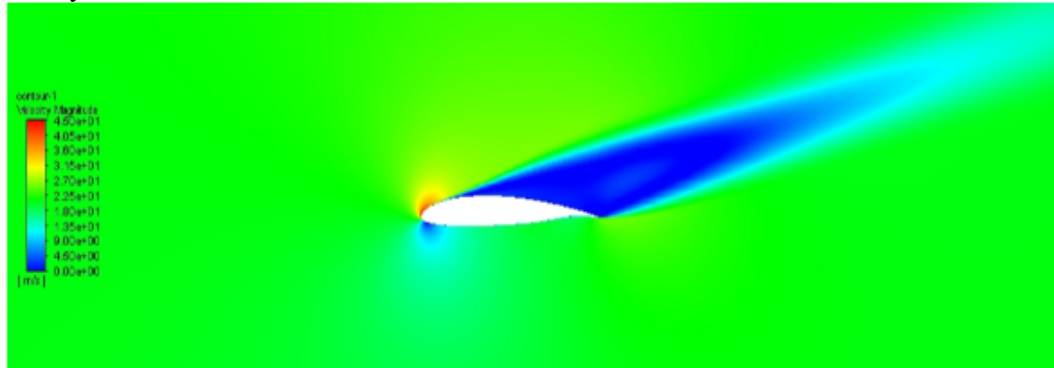


Fig 57: Velocity contour at $\alpha = 18^\circ$

Values of C_l and C_d with their corresponding angle of attack is given in the table below:

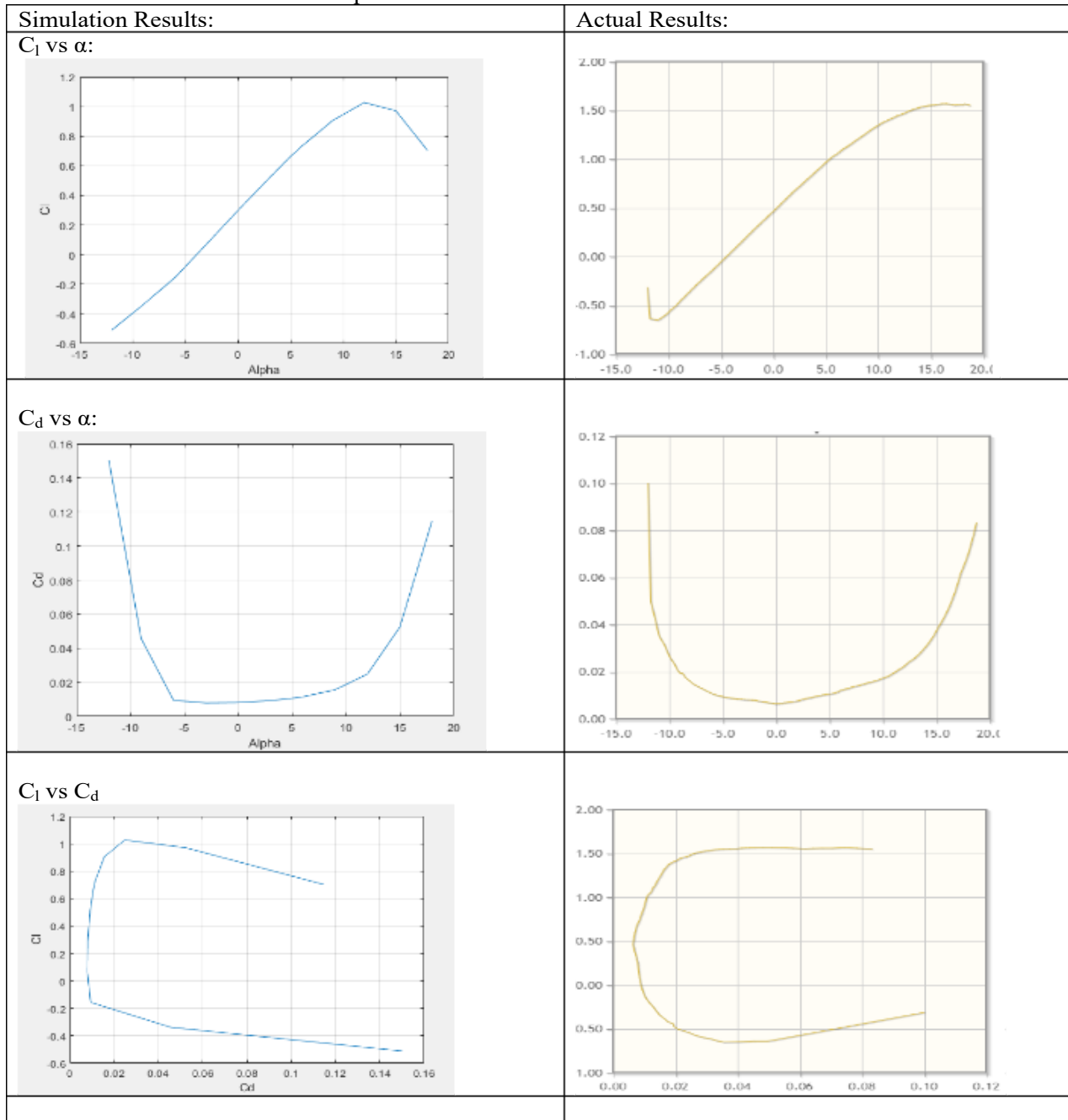
Table 3: C_l and C_d values with corresponding α

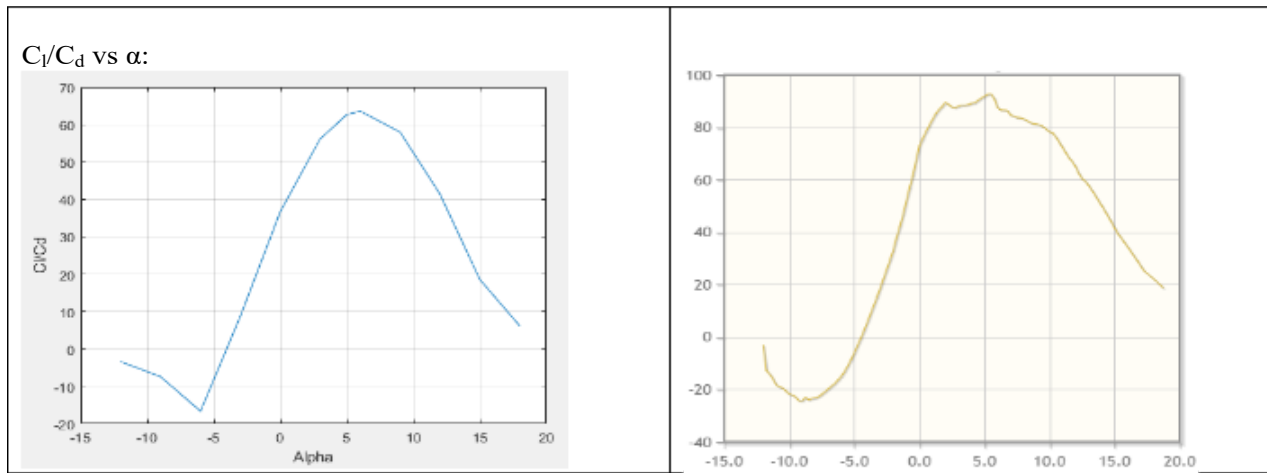
α ($^\circ$)	C_l	C_d
-12	-0.51157188	0.15012936
-9	-0.33837816	0.045593001
-6	-0.1567446	0.0094047
-3	0.06920106	0.007876064
0	0.29730332	0.008094392
3	0.51946902	0.00924464
5	0.66266114	0.010578252
6	0.72792315	0.011448846
9	0.90545964	0.015616245
12	1.0270441	0.024801711
15	0.97100967	0.052284714
18	0.70317912	0.11458721

12. Verification of Ansys Simulations

With these values, we can plot various graphs like C_l vs α , C_d vs α , C_l/C_d vs α by using the ‘plot’ function in the MATLAB. So, for verifying our results, we will compare these graphs from the graphs taken from aerofoiltools.com database.

Table 4: Comparison of Simulation Results vs XFOIL Results





12.1 Analysis

25 Well, we can say that at least the curves of the plots are similar to the actual case. But, on a true note, these values are more accurate than we were expecting.

41 From the above plots and results, one thing we can observe is the simulation results are quite consistent at low values of α , that is, between α of -10° to $+10^\circ$, simulation results are more consistent than for the higher values of α .

The plots that we took from the aerofoiltools.com are made using the XFOIL Software. So, one question that may arise is that why are simulations of Ansys and XFOIL don't match. The answer is that both of these software uses different methods for computing. XFOIL uses potential flow force equations while Ansys uses RANS (Reynold's Averaged Navier-Stokes) equations.

Still, it is a topic of debate that which one of these software gives accurate results. Some people believe that RANS is high fidelity method, meaning that the degree of exactness of RANS is higher than potential flow equations, while others say that XFOIL results matches better than the Ansys. Here, I would like to point out that the XFOIL is specifically made for testing at subsonic speed.

So, we can conclude that for testing at low values of Re ($< 1,500,000$), XFOIL must be preferred while at higher values, Ansys must be preferred.

If we actually have to verify these results, we can do so by wind tunnel testing. Unfortunately, there weren't any existing wind tunnel test results for this aerofoil and so it is impossible to verify the results with 100 percent accuracy, but still we can get a decent idea of typical values of C_L and C_d at different values of α .

One most interesting thing to note is that in C_L/C_d vs α curve, max value of C_L/C_d is around 64, which is almost equal to our best glide ratio (Glide Ratio can also be calculated as the ratio of C_L and C_d value. This observation can further verify and attest to our simulation results.

13. Lift and Drag Coefficients at different chord length

We will now analyse the same aerofoil at different chord length. In a sailplane, by varying the dimensions of the wing, its Aspect Ratio (AR) can be changed. In aerodynamics, this AR is defined as ratio of the wingspan to chord length of the wing. So, AR is an important parameter if we are concerned about the designing of high-performance sailplanes.

If we assume the aerofoil DU 84-132 is used as the cross section of whole wing, then by changing its chord ⁴⁴ we are actually changing its Aspect Ratio. Therefore, the study in the following section can shed some light on the current design of the ASW 22 BL wing structure and if it can be improved further.

We basically followed the same steps as mentioned above for different body scaling according to the chord length requirements. We will simulate every aerofoil at same altitude and airspeed to draw the comparison between them.

13.1 Results

For current design chord length (0.6939948m, AR = 38.3)

Static Pressure Contour:

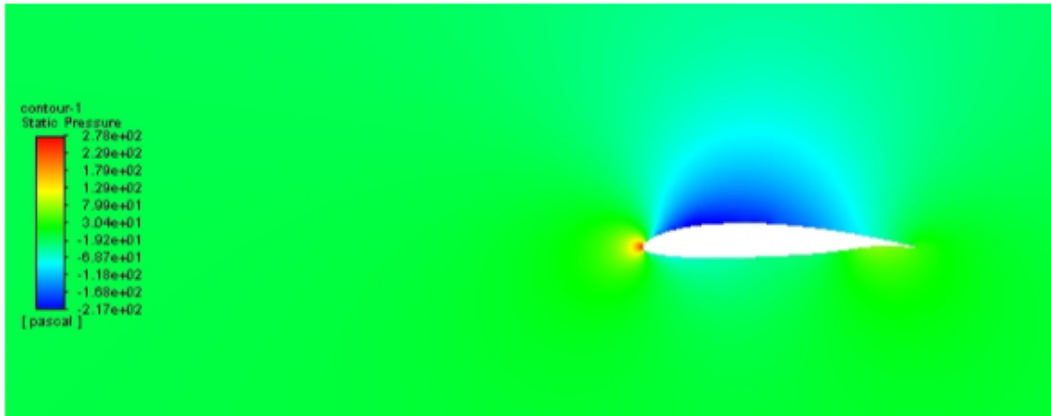


Fig 58: Static pressure contour at AR = 38.3

Velocity Contour:

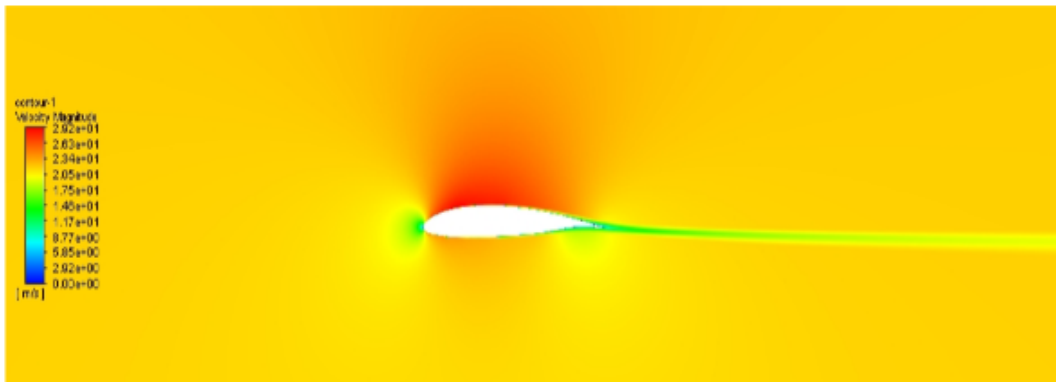


Fig 59: Velocity contour at AR = 38.3

For chord length 0.632857142m (AR = 42)

Static Pressure Contour:

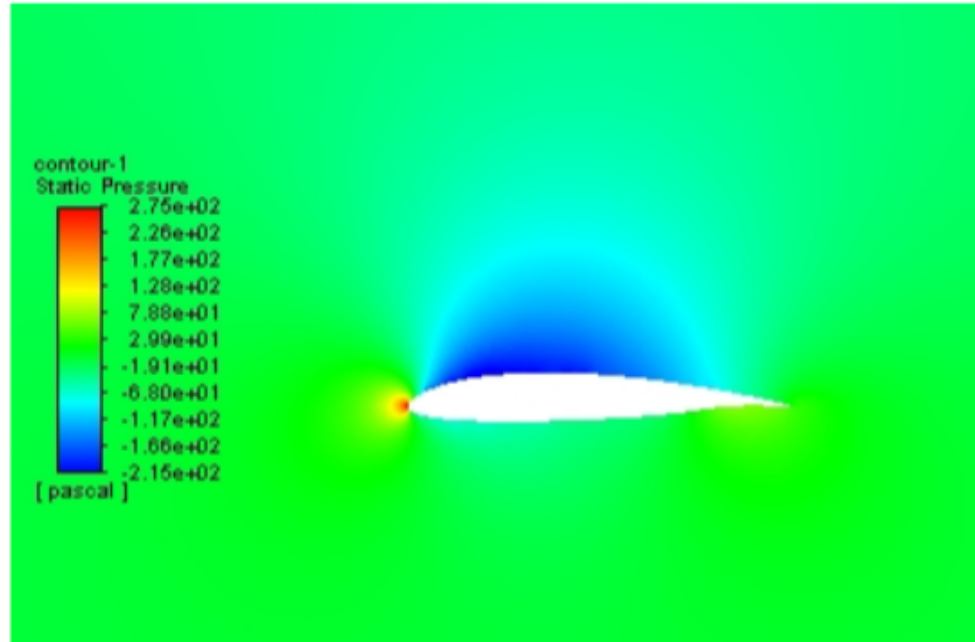


Fig 60: Static pressure contour at AR = 42

Velocity Contour:

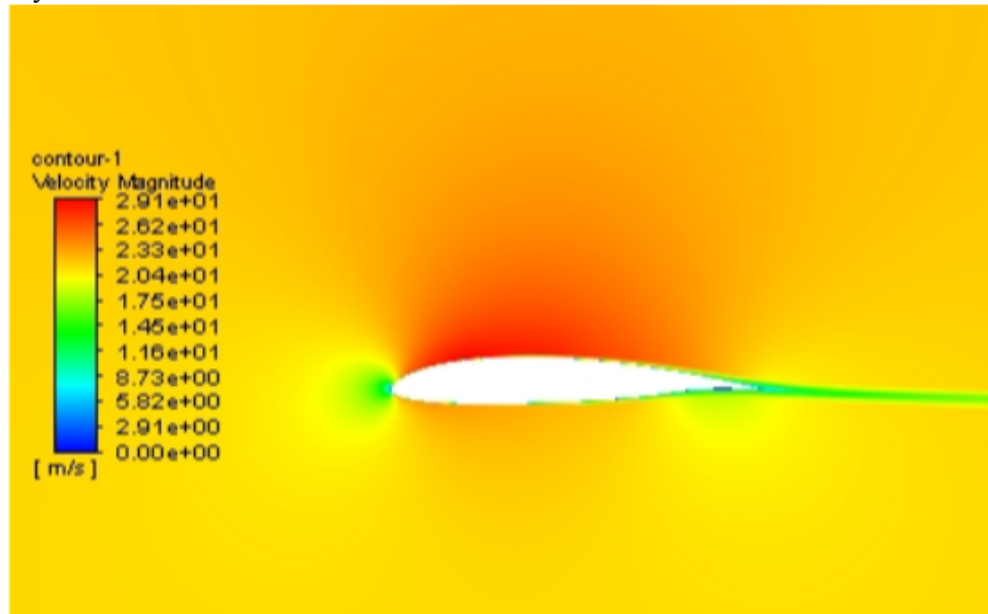


Fig 61: Velocity contour at AR = 42

For chord length 0.759428571m (AR = 35)

Static Pressure Contour:

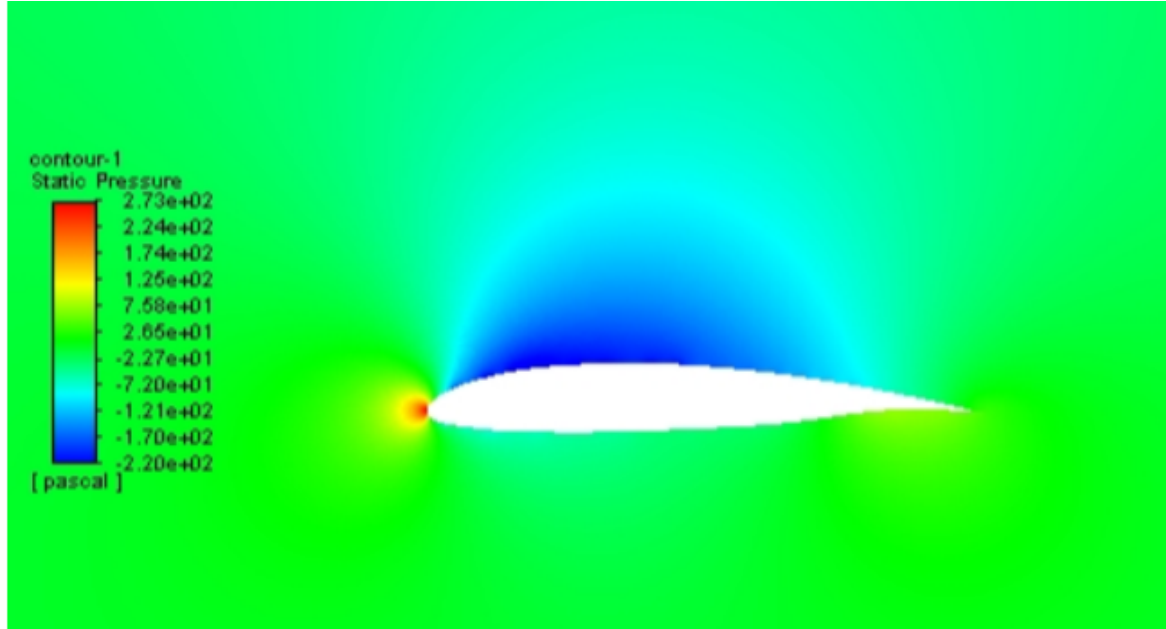


Fig 62: Static pressure contour at AR = 35

Velocity Contour:

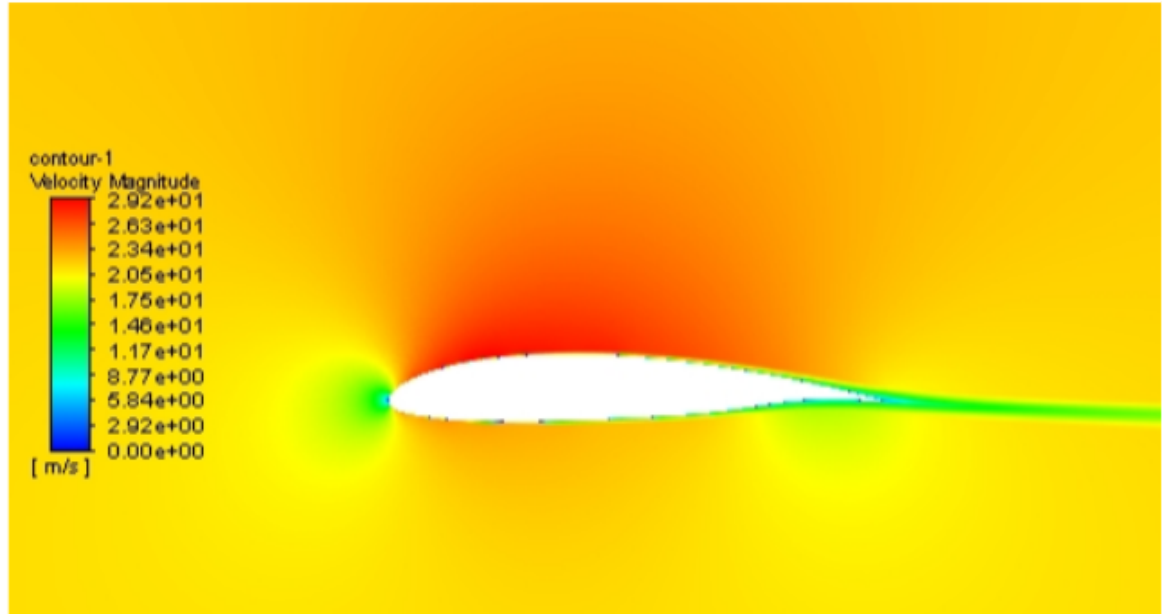


Fig 63: Velocity contour at AR = 35

For chord length 0.830625m (AR = 32)

Static Pressure Contour:

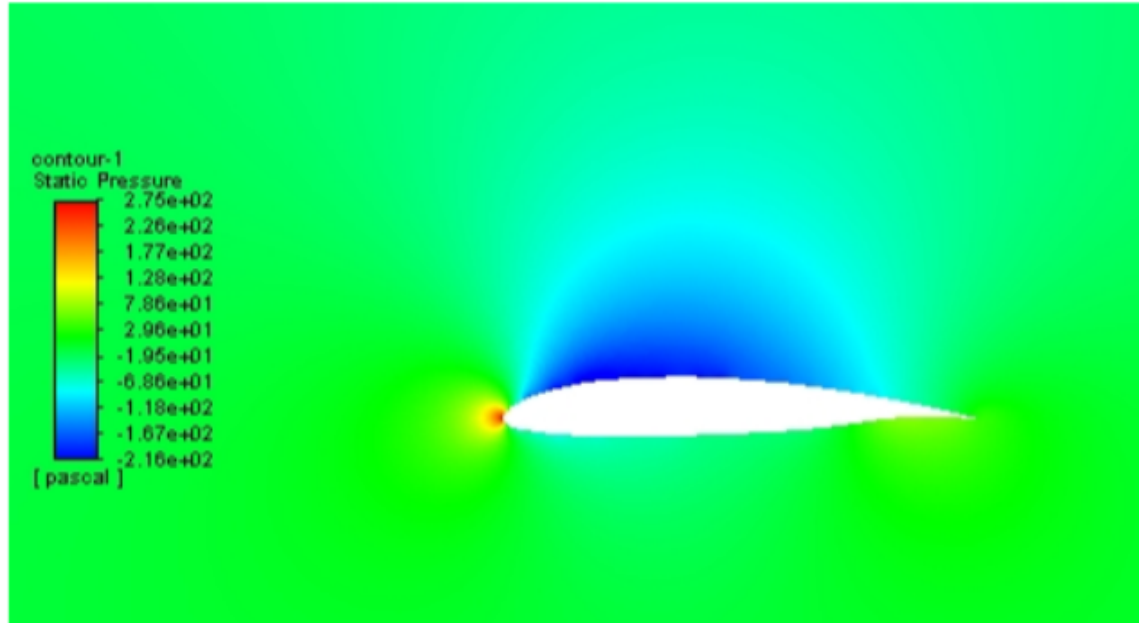


Fig 64: Static pressure contour at AR = 32

Velocity Contour:

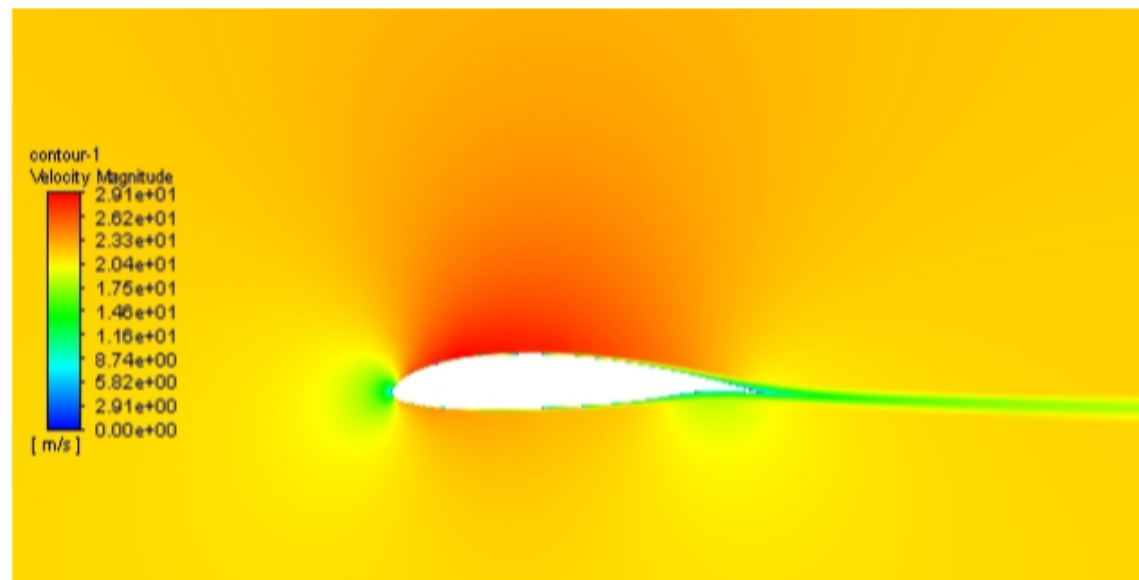


Fig 65: Velocity contour at AR = 32

13.2 Analysis

These contours don't seem much different from each other. So, to analyse our results, we will look at the C_l and C_d values at these chord lengths in the following table:

Table 5: C_l and C_d at different chord length

Chord Length (m)	Aspect Ratio	C_l	C_d	Glide ratio (C_l/C_d)
0.693994800	38.3	0.297081	0.008095	36.70098
0.632857142	42	0.27032	0.007467	36.20156
0.759428571	35	0.344003	0.008847	38.88311
0.830625000	32	0.357718	0.009515	37.59607

We can observe that as the AR is increased above the designed value, C_l and C_d are decreased but the change in C_d is greater because the value of glide ratio is decreased.

But if we lower the AR to 35 (and increase the chord length), both C_l and C_d are increased but the increase in C_l is greater than that in C_d , because we see that the corresponding value of glide ratio is increased.

Now if we further lower the AR to 32, both of the coefficients would increase in value but it won't be of use to us because overall glide ratio is decreased.

14. Conclusion

⁴¹ From the above results, we can come to the conclusion that if we want to further optimize the design of ASW 22 BL sailplane, it won't do any good to increase the aspect ratio, but we have to decrease this value. Therefore, further experiments can be done on the high-performance sailplane on basis of this report because there still exists a possibility to further optimize the design of this sailplane.

We also the importance of the glide ratio parameter. While designing a sailplane, our objective is to maximize this value. These days modern sailplanes can achieve a glide ratio of up to 70 and ⁴² with the passage of time it will only increase. But as these sailplanes offer greater performance, they obviously have a high selling price. Therefore, it will benefit a production company to make their effort in optimizing and relaunching the old sailplanes because the selling price of these sailplanes would be lower as compared to the hyper modern sailplanes while the performance would still be comparable.

²³ We can optimize the design of this aircraft by not only changing the dimensions and geometry of the wing but by also improving the material ⁴⁴ of the sailplane by which it is made. Research is already being going for making new composites to employ them in the making of the aircraft. So ⁴⁵ probably in less than a decade, we will be able to see a sailplane that will cross the glide ratio of 100 mark.

15. Contributions:

Of course, both students have contributed equally and have equal understanding of concept, still Yash worked in some areas while Srajan worked on other areas. Individual Contribution Report by each of us is mentioned below:

15.1 Individual contribution report by Yash: -

Evolution of Aerofoils sections have been covered thoroughly covering all the important aspects of aerofoils. In this section, the focus is mainly on how the aerofoils have been developed so far from the 19th century till the present time. The very first aerofoil developed was Lilienthal aerofoil which was invented by a scientist named Lilienthal in the year of 1894. It covered a distance of 80m from a height of 15m. Although it has been a big achievement but ²² there were some issues regarding the lift and moment curves. In the coefficient of lift vs coefficient of drag curve, below coefficient of lift of 0.5 there was a rapid increase in coefficient of drag which clearly indicated a separation of flow over the lower side of aerofoil. In lift and moment characteristics curves, there was also the lift breakdown at alpha of 15degrees Goe441 aerofoil represented the Vampyr sailplane invented in the year 1921 by Academics Flying Group. In this case in lift and moment characteristics curve, there was also the lift breakdown at 15degrees. And in coefficient of lift vs coefficient of drag curve, at coefficient of lift of almost equal to 0, there was already the drag present Up till now all the aerofoils were developed ²³ for fully turbulent boundary layer but during the 1940s the concept of laminar aerofoils came into being. The NACA 633618 which was developed in the year 1938, its wings required an extremely low surface roughness and an accurate shape of the aerofoil contour. It was difficult to achieve with the wooden kind of structure in the early fifties but further due to weight the torsion D-box was strained to less than the first 30% of wing chord followed by a covering, clearly terminating the laminar boundary layer. In the coefficient of lift vs coefficient of drag curve, the drag polar shifted toward left for laminar boundary layer resulting in loss of drag which a great achievement at that time. Then came the R. Eppler aerofoil of the Phoenix sailplane in the year 1957. The maximum lift coefficient was ²⁶ a result of the large curvature on the rear of the upper aerofoil side which was fixing the ²⁶ flow separation within the high curvature region up to very large angles of attack. The very low drag at lift coefficients from 0.5 to ⁹ 0.9 ²³ is a result of the long extent of laminar flow on both sides of the aerofoil. At higher and ⁴⁶ lower lift coefficients the drag is increasing due to reduced extent of laminar flow on the ⁷ upper side respectively on the lower side of the aerofoil. A very successful and appreciable work on aerofoil design and testing had been performed by F. X. Wortmann and D. Althaus. One of their first well known aerofoils is the FX 61-163, designed in 1961. At cruise condition a clear advantage is visible but at medium lift coefficients there was the higher drag compared to the Phoenix aerofoil which can result in a decreased maximum glide ratio. The Wortmann aerofoil FX 62-K-131/17, ²³ is one of the early camber flap aerofoils used for the first time at D 36 of the Academic Flight Group of Darmstadt and later with slight modifications and improvements in many other sailplanes. The coefficient of lift vs coefficient of drag curve shows the typical effect of flap deflection on the laminar drag bucket and also the very low drag of this aerofoil with values below 0.005 for cruise conditions.

Drags and their contributions⁶ have been mentioned for the aerofoils. The main drags contribution was from the induced drag, profile drag, fuselage drag, and tailplane drag. The largest contribution is due to the wing; at low speed due to induced drag and at high speed due to profile drag.²⁷ The below figure shows the absolute minimum induced drag can be realized within 0.96% at all lift coefficients. Apart from that, the winglet aerofoils have been designed for low profile drag in their operational region of lift coefficients, obtained by 100% fully laminar flow on the lower surface and 50% on the upper surface of the aerofoil. Also, the ample reserve to separation for yaw has been applied, at significantly low speeds while circling in thermals.²⁶ Profile drag is caused by the separation of boundary layer resulting into wakes formation. It depends on the extent of the laminar boundary layer on the lower and upper surfaces of the aerofoils and on aerofoil thickness. The wing aerofoil has laminar flow up to 95% of the chord on the lower surface at the high-speed 0degree flap deflection, and up to 75% of the chord on the upper surface at the low-speed 20 degrees flap deflection, as indicated by the pressure distributions in the above figure. The lower and upper surface flap gaps have been sealed by flexible mylar strips. It allows and permits the boundary layer on the lower surface to remain laminar beyond the flap hinge position at the 0degree flap deflection up to 95%. On the upper surface the sealing prevents low-pressure peaks and subsequent steep pressure gradients on the flap at 20 degrees deflection, thus postponing separation. Consequently, the profile drag becomes very low over a large range of lift coefficients. Fuselage drag as clear by its name depends mainly on fuselage thickness, contraction behind the cockpit, and streamline shaping. Fuselage frontal area should be very minimal. Contraction behind the cockpit and the corresponding pressure gradient is restricted because of flow separation when the boundary layer on the fuselage is completely turbulent, for example when flying in rain with heavy thunderstorms. For an undisturbed boundary layer development, continuity of curvature is required in flow direction. It is guaranteed by deriving the top, bottom, and line of largest width from aerofoil shapes.

¹⁷ A significant finding is that the fuselage length can be increased by 0.3 metres without any drag increase, as illustrated by the accumulative development of the drag coefficient on a rotationally symmetrical body in the figure. Transition occurs at 33% of the original fuselage length, and thus the total drag is found at the tail.³¹ This result grants the probability for improved crashworthiness measures as a longer crumpling nose cone and keeping the pilot's feet out of this zone.

MATLAB Code Analysis section has been covered of the both the sailplanes, i.e., Diana-3 and ASW-22BL. All the technical parameters have been mentioned like wingspan, wing area, Oswald efficiency factor, drag coefficient factor, maximum and minimum wing loading, etc. The output results have been taken out for true airspeed in fps and knots, calibrated airspeed in knots, best glide angle in radians and degrees, best value of drag and lift, dynamic pressure, best value of drag and lift coefficients, best glide ratio, range, sink rate and endurance. The figures or curves that have been deduced are L/D vs KCAS, L/D vs TAS, L/D vs Cl, parasite, induced and total drag curves resulting in velocity for minimum drag curves and drag polar curves.⁴⁵ Further the results have been verified by the simulation works.

15.2 Individual contribution report by Srajan: -

I firstly worked on the aerodynamics and performance aspects of the gliders in depth. Under this, I came to know about the factors that affect the performance of a glider during flight. These are: altitude, temperature, wind and weight. Understanding the factors of temperature and wind is important as we have to consider these atmospheric changes while designing any aircraft because pilots have to fly the aircraft under these conditions. And then they also have to know about the altitude at which it is safe enough to glide a sailplane with maximum performance. Weight of the sailplane must be optimum to maximize the L/D Ratio.

This L/D ratio is what led me to study the aerodynamics of the aircraft. I have written about it in detail in the report about how the gliders stay aloft for hours even without an engine to provide thrust. To summarize it in one line, they basically use the horizontal component of lift and weight to glide forward.

Coming back to the glider performance, I have also written about other factors which can affect the performance of sailplane. These are: rate of climb, placards and ballast. Rate of climb depends on the strength of the ground-launching equipment in case of sailplanes as they cannot climb on their own unlike the motored sailplanes. In the motored sailplanes, it directly depends on the motor or the engine they are using. These ground launching equipment are in the form of a tow plane and a winch. So, the more powerful they will be the better. Another important concept is of water ballast. They are used to increase weight of the glider while in flight as it provides more forward force.

I also discussed in brief about the different types of gliders which are paragliders, hand gliders, and high-performance gliders and made the comparison table of the same.

I spent my major amount of time in doing Ansys simulations and learned a great deal about it in the process. If given more time, I would have generated better results. I learned about it in my regular classes but still invested more time in learning it by watching tutorial videos online and reading the online forums and discussions. In this project, I used Spalart Allmaras method to compute C_l and C_d values due to its better computational time. But it is not the best model to calculate drag values as discussed in the project. K-omega SST model is best but of course, the time to compute with this method is much higher as compared to the model used. A point to be noted however is that the Spalart Allmaras model is very good if we are simulating at 0-degree angle of attack. So, keeping this in mind I performed more simulations to see how the lift and drag values are affected by changing the dimensions of the aerofoil. By doing this, I found very interesting results which are thoroughly discussed in the report.

Finally, I arrived at the conclusion that there still are optimizations to be made in the ASW 22 BL sailplane and that it would be beneficial for its production company.